"In presenting the dissertation as a partial fulfillment of the requirements for an advanced degree from the Georgia Institute of Technology, I agree that the Library of the Institution shall make it available for inspection and circulation in accordance with its regulations governing materials of this type. I agree that permission to copy from, or to publish from, this dissertation may be granted by the professor under whose direction it was written, or, in his absence, by the dean of the Graduate Division when such copying or publication is solely for scholarly purposes and does not involve potential financial gain. It is understood that any copying from, or publication of, this dissertation which involves potential financial gain will not be allowed without written permission.

_____"

HEAT TRANSFER TO LIQUID METALS FLOWING TURBULENTLY IN A PIPE

A THESIS

Presented to

the Faculty of the Graduate Division

by

Duane LeRoy Franklet

In Partial Fulfillment

of the Requirements for the Degree

Doctor of Philosophy in the School of Chemical Engineering

Georgia Institute of Technology

June 1958

50
127

HEAT TRANSFER TO LIQUID METALS FLOWING TURBULENTLY IN A PIPE

Approved:

Date Approved by Chairman: July 28, 1958

ACKNOWLEDGMENTS

The author wishes to express his appreciation to the late Dr. J. M. DallaValle for his encouragement and counsel; to Dr. W. B. Harrison for his advice and cheerful guidance; to Mr. O. V. Hefner, who assisted with the programming; to Mr. R. J. Hefner, who assisted with the programming and who rendered invaluable assistance throughout this study; and to the many kind people associated with Rich's Computer Center.

The author is grateful to the Socony-Vacuum Oil Company for the Socony-Vacuum Fellowship in Chemical Engineering during the academic year of 1956-57 and to the Phillips Petroleum Company for the Phillips Petroleum Fellowship in Chemical Engineering during the academic year of 1957-58.

The author's gratitude to his wife is immeasurable.

TABLE OF CONTENTS

NOMENCLATURE

Symbol	Definition	Units
A	Surface area, $2\pi R\Delta x$	$ft.^2$
A^+	Constant	
Cp	Specific heat at constant pressure	$Btu/lb._m\,^oF$
D	Diameter	ft.
f	Moody friction factor, $8\ g_c\ \tau_w/\ u^2_m$	
g_c	Conversion factor	$ft.\ lb._m/hr.^2\ lb._f$
h	Coefficient of heat-transfer	$Btu/hr.\ ft.^2$
k	Thermal conductivity of fluid	$Btu/hr.\ ft.\ ^oF/ft.$
K	Constant	
M	Parameter, $1 - 1/\sigma\ Pr$	
Nu	Nusselt number, hD/k	
p	Pressure	$lb._f/ft.^2$
Pe	Peclet number, $Re \cdot Pr$	
Pr	Prandtl number, ν/α	
Pr'	Parameter, σPr	
q	Heat flux	Btu/hr.
r	Radical distance from pipe center	ft.
R	Radius of pipe	ft.
R^+	Dimensionless radius of pipe, $\frac{1}{2}\ Re\lambda$	

Symbol	Definition	Units
Re	Reynolds number, Du_m/ν	
t	Temperature of fluid at any point	^oF
T^*	Friction temperature, $q_w/\rho C_p A_w\sqrt{g_c \tau_w/\rho}$	^oF
u	Axial velocity component	ft./hr.
u^+	Dimensionless velocity, $u/\sqrt{g_c \tau_w/\rho}$	
u_T^+	Dimensionless velocity at the lower limit of the turbulent core	
v	Radial velocity component	ft./hr.
x	Distance in the axial direction	ft.
y	Radial distance from pipe wall, R - r	ft.
y^+	Dimensionless radial distance from pipe wall, $\sqrt{g_c \tau_w/\rho}\ y/\nu$	
GREEK		
α	Thermal diffusivity of fluid	$ft.^2/hr.$
Δ	Finite difference	
ϵ_H	Eddy diffusivity of heat-transfer	$ft.^2/hr.$
ϵ_M	Eddy diffusivity of momentum-transfer	$ft.^2/hr.$
θ	Temperature at pipe wall minus fluid temperature at any point, $t_w - t$	^oF
λ	Parameter, $\sqrt{f/8}$	
ν	Kinematic viscosity of fluid	$ft.^2/hr.$
ξ	Dummy variable	
ρ	Density of fluid	$lb._m/ft.^3$

σ	Ratio of eddy diffusivities of heat and momentum, $\varepsilon_H/\varepsilon_M$	
τ	Shear stress at any point	$lb._f/ft.^2$

SUBSCRIPTS

c	Centerline
m	Bulk mean
w	Wall
r	Any radius

SUPERSCRIPTS

'	Fluctuating component
-	Temporal mean

LIST OF TABLES

LIST OF FIGURES

SUMMARY

Many theoretical and experimental investigations during the past decade have dealt with heat transfer in liquid metals. It was the purpose of this study to further examine predictions of heat transfer coefficients for liquid metals by the momentum-heat transfer analogy methods.

This investigation employed essentially the same development as proposed by Boelter, Martinelli and Jonassen, (Transactions of the American Society of Mechanical Engineers, 63, 447-55, 1941). The flow field was divided into three regions as follows: (a) Laminar layer, where the eddy diffusivities are considered to be negligible. (b) Buffer layer, where the eddy and molecular diffusivities are of the same order of magnitude. (c) Turbulent core, where only the eddy diffusivities are considered to be effective. The dimensionless universal velocity distribution as proposed by von Karman (Transactions of the American Society of Mechanical Engineers, 61, 705-10, 1939) was used for smooth pipe. In prior utilizations of the analogy the boundary limits between the laminar layer, buffer layer and turbulent core coincided with the division of the flow field made by von Karman. In this investigation, the lower limit of the turbulent core was approximately determined from the existing experimental heat-transfer data for liquid metals to be $y^+ = 70$. To simulate the roughness observed by Brown, Short, and Amstead (Transactions

of the American Society of Mechanical Engineers, 79, 279-86, 1957) in their experimental investigation of heat transfer to mercury, the constants and range of the velocity distribution equations were varied. Employing this variation, it was found that Martinelli's theory would predict a six to twelve per cent increase in the heat-transfer coefficient for Pr = 0.01; thus increasing the discrepancy between his theory and the experimental data.

In this analysis the ratio of the diffusivities of heat to momentum was included as a parameter in the mathematical development, although for the final numerical computations a value equal to one was utilized due to the uncertainty of this term. The results may easily be re-evaluated for a mean value of the ratio different from unity.

Using the step-like functions for the diffusivities of heat and momentum and the choice of the buffer-layer limit, $y^+ = 70$, good agreement is obtained between the predictions of this investigation and the experimental data for liquid metals. In addition, improved agreement is obtained for normal fluids, when the more accurate velocity distribution of van Driest (Heat Transfer and Fluid Mechanics Institute, University of California, 1955) is employed.

CHAPTER 1

INTRODUCTION

Many theoretical and experimental investigations during the past decade have dealt with heat transfer in liquid metals. It was the purpose of this study to further examine predictions of heat-transfer coefficients for liquid metals by the momentum-heat transfer analogy.

The development and use of the analogy methods, together with various other approaches to the calculation of heat transfer coefficients, is reviewed by Summerfield (1), Jakob (2) and Jakob (3). Additional references not contained in the above reviews or cited in this work are also contained in the bibliography.

The present form of the analogy evolved from the postulate that an intermediate or buffer layer, in which the viscous and turbulent terms are of the same order of magnitude, existed between a laminar sublayer and a turbulent core. This concept was introduced independently by Eagle and Ferguson (4) and von Karman (5). It was not developed until von Karman (6) proposed to use Nikuradse's velocity data for smooth pipe in the form of the dimensionless universal velocity distribution as follows:

$$u^+ = y^+ \qquad 0 \leq y^+ \leq 5 \qquad (1a)$$

$$u^+ = -3.05 + 5.0 \ln y^+ \qquad 5 \leq y^+ \leq 30 \qquad (1b)$$

$$u^+ = 5.5 + 2.5 \ln y^+ \qquad 30 \leq y^+ \qquad (1c)$$

Boelter, Martinelli and Jonassen (7) extended von Karman's analysis and derived an expression for the temperature distribution in a fluid inside of a cylindrical pipe being heated or cooled with constant heat flux. Employing this temperature distribution, a relation for the Nusselt number was obtained. To correct for the assumption of constant physical properties, the apparent variation of the parameter y^+ with the ratio of wall viscosity to viscosity at the edge of the laminar layer and Reynold's number was obtained from experimental data. In addition, the friction factors were calculated from the mean conditions in the laminar layer. These corrections permit prediction of heat-transfer coefficients for fluids other than liquid metals with an accuracy comparable to the empirical relationships.

Martinelli (8) pointed out that the molecular conductivity of heat cannot be neglected in the turbulent core when the Prandtl number is considerably less than one, i.e., the molecular conduction is of the same order of magnitude as the eddy diffusivity of heat. Liquid metals comprise this group. Retaining the molecular conduction of heat in the turbulent core, he altered the previous calculations for ordinary fluids. Although Martinelli assumed a constant wall temperature for his calculations, his assumption that $\left(\frac{\partial t}{\partial x}\right)_r = \left(\frac{\partial t}{\partial x}\right)_{avg}$ is tantamount to assuming constant heat flux. The question as to whether the molecular shear should be considered in the turbulent core is discussed in Appendix I. It was concluded that the term was negligible in this region.

Lyon (9) utilized Martinelli's model and obtained numerical solutions without introducing the approximation of linear transverse heat transfer. The predicted Nusselt numbers were slightly less than those obtained by Martinelli. He also proposed a simplified equation which approximated his own calculations and Martinelli's complex relation.

In order to determine the temperature distribution and hence the heat-transfer coefficient, the analogy assumes a ratio between the eddy diffusivities of momentum and heat, ε_M and ε_H, defined as follows:

$$\sigma = \frac{\varepsilon_H}{\varepsilon_M} \tag{2}$$

The dimensionless universal velocity distribution as proposed by von Karman is used to determine ε_M, and hence ε_H for a given σ. Nusselt numbers can then be readily calculated. These approximate velocity relations, Equations 1a, 1b, and 1c yield a reasonably good correlation with the data. Other investigators have chosen to develop velocity and/or heat-transfer relationships. Among the outstanding of these are Deissler and Eian (10); Deissler (11); Rannie (12); Reichardt (13) and (14); and van Driest (15).

This investigation employs essentially the same development as proposed by Boelter, et al. The flow field is divided into three regions as follows:

(a) Laminar layer - The eddy diffusivities are considered to be negligible.

(b) Buffer layer - The eddy and molecular diffusivities are of the same order of magnitude.

(c) Turbulent core - Only the eddy diffusivities are considered to be effective.

The dimensionless universal velocity distribution as proposed by von Karman is used for smooth pipe. For rough pipe, the constants and range of the equations vary; hence Equations 1a, 1b and 1c will be designated in the notation:

$$u^+ = y^+ \qquad 0 \leq y^+ \leq y_1^+ \qquad (3a)$$

$$u^+ = C_1 + C_2 \ln y^+ \qquad y_1^+ \leq y^+ \leq y_2^+ \qquad (3b)$$

$$u^+ = C_3 + C_4 \ln y^+ \qquad y_2^+ \leq y^+ \qquad (3c)$$

In prior utilizations of the analogy the boundary limits between the laminar layer, buffer layer and turbulent core coincided with Equations 1a, 1b and 1c. In this investigation, the lower limit of the turbulent core, y_T^+, will be approximately determined from the existing experimental heat-transfer data for liquid metals. Note, however, that the range of Equations 3a, 3b and 3c is not altered by this choice of the buffer layer. The conditions imposed on each region by Boelter, et al., Martinelli, and this investigation are compared in Table I.

Chapter II develops the necessary equations for calculating the temperature distribution and the heat-transfer coefficient in the form of the Nusselt number. The accuracy of the dimensionless universal velocity

Table 1. Assumptions Employed Compared with the Work of Boelter, et al., and Martinelli

Region	Laminar Layer		
Reference	Boelter, et al., (7)	Martinelli (8)	This Investigation
Experimental Velocity Distribution	$u^+ = y^+$ $0 \leq y^+ \leq 5$	$u^+ = y^+$ $0 \leq y^+ \leq 5$	$u^+ = y^+$ $0 \leq y^+ \leq 5$
Shear	$\tau = \tau_w$	$\tau = \tau_w$	$\tau = \tau_w$
Shear Equation	$\frac{\tau}{\rho} = \nu \frac{du}{dy}$	$\frac{\tau}{\rho} = \nu \frac{du}{dy}$	$\frac{\tau}{\rho} = \nu \frac{du}{dy}$
Eddy Diffusivity	$\varepsilon_M = \varepsilon_H = 0$	$\varepsilon_M = \varepsilon_H = 0$	$\varepsilon_M = \varepsilon_H = 0$
Heat Flux	$\frac{q}{A} = \frac{q_w}{A_w}$	$\frac{q}{A} = \frac{q_w}{A_w}$	$\frac{q}{A} = \frac{q_w}{A_w}$
Heat Flux Equation	$\frac{q}{A} = -k \frac{dt}{dy}$	$\frac{q}{A} = -k \frac{dt}{dy}$	$\frac{q}{A} = -k \frac{dt}{dy}$
Region	Buffer Layer		
Reference	Boelter, et al. (7) and Martinelli (8)	This Investigation	
Experimental Velocity Distribution	$u^+ = -3.05 - 5.00 \ln y^+$ $5 \leq y^+ \leq 30$	$u^+ = C_1 + C_2 \ln y^+$ $5 \leq y^+ \leq y_2^+$	$u^+ = C_3 + C_4 \ln y^+$ $y_2^+ \leq y^+ \leq y_T^+ = 70$
Shear	$\tau = \tau_w$	$\tau = \tau_w$	$\tau = \tau_w \left(1 - \frac{y}{r_w}\right)$

(Continued)

Table 1. Continued

Region	Buffer Layer		
Reference	Boelter, et al. (7) and Martinelli (8)	This Investigation	
Shear Equation	$\frac{\tau}{\rho} = (\nu + \varepsilon_M)\frac{du}{dy}$	$\frac{\tau}{\rho} = (\nu + \varepsilon_M)\frac{du}{dy}$	$\frac{\tau}{\rho} = (\nu + \varepsilon_M)\frac{du}{dy}$
Eddy Diffusivity	$\varepsilon_M = \frac{\frac{\tau}{\rho}}{\frac{du}{dy}} - \nu$ $\varepsilon_H = -\frac{\frac{q}{A\, cp\rho}}{\frac{dt}{dy}} - a$	$\varepsilon_M = \frac{\frac{\tau}{\rho}}{\frac{du}{dy}} - \nu$ $\varepsilon_H = -\frac{\frac{q}{A\, Cp\, \rho}}{\frac{dt}{dy}} - a$	$\varepsilon_M = \frac{\frac{\tau}{\rho}}{\frac{du}{dy}} - \nu$ $\varepsilon_H = -\frac{\frac{q}{A\, cp\, \rho}}{\frac{dt}{dy}} - a$
Heat Flux	$\frac{q}{A} = \frac{q_w}{A_w}$	$\frac{q}{A} = \frac{q_w}{A_w}$	$\frac{q}{A} = \frac{q_w}{A_w}\left(1 - \frac{y}{r_w}\right)$
Heat Flux Equation	$\frac{q}{A\, C_p\, \rho} = -(a + \varepsilon_H)\frac{dt}{dy}$	$\frac{q}{A\, Cp\, \rho} = -(a + \varepsilon_H)\frac{dt}{dy}$	$\frac{q}{A\, Cp\, \rho} = -(a + \varepsilon_H)\frac{dt}{dy}$
Region	Turbulent Core		
Reference	Boelter, et al. (7)	Martinelli (8)	This Investigation
Experimental Velocity Distribution	$u^+ = 5.5 + 2.5 \ln y^+$ $30 \leq y^+$	$u^+ = 5.5 + 2.5 \ln y^+$ $30 \leq y^+$	$u^+ = C_3 + C_4 \ln y^+$ $70 = y_T^+ \leq y^+$

(Continued)

Table 1. Concluded

Region	Turbulent Core		
Reference	Boelter, et al.(7)	Martinelli (8)	This Investigation
Shear	$\tau = \tau_w \left(1 - \frac{y}{r_w}\right)$	$\tau = \tau_w \left(1 - \frac{y}{r_w}\right)$	$\tau = \tau_w \left(1 - \frac{y}{r_w}\right)$
Shear Equation	$\frac{\tau}{\rho} = \varepsilon_M \frac{du}{dy}$ $\varepsilon_M = \frac{\frac{\tau}{\rho}}{\frac{du}{dy}}$	$\frac{\tau}{\rho} = \varepsilon_M \frac{du}{dy}$ $\varepsilon_M = \frac{\frac{\tau}{\rho}}{\frac{du}{dy}}$	$\frac{\tau}{\rho} = \varepsilon_M \frac{du}{dy}$ $\varepsilon_M = \frac{\frac{\tau}{\rho}}{\frac{du}{dy}}$
Eddy Diffusivity	$\varepsilon_H = - \frac{\frac{q}{A\, Cp\, \rho}}{\frac{dt}{dy}}$	$\varepsilon_H = - \frac{\frac{q}{A\, Cp\, \rho}}{\frac{dt}{dy}}$	$\varepsilon_H = - \frac{\frac{q}{A\, Cp\, \rho}}{\frac{dt}{dy}}$
Heat Flux	$\frac{q}{A} = \frac{q_w}{A_w}\left(1 - \frac{y}{r_w}\right)$	$\frac{q}{A} = \frac{q_w}{A_w}\left(1 - \frac{y}{r_w}\right)$	$\frac{q}{A} = \frac{q_w}{A_w}\left(1 - \frac{y}{r_w}\right)$
Heat Flux Equation	$\frac{q}{A\, Cp\, \rho} = - \varepsilon_H \frac{dt}{dy}$	$\frac{q}{A\, Cp\, \rho} = - (\alpha + \varepsilon_H) \frac{dt}{dy}$	$\frac{q}{A\, Cp\, \rho} = - \varepsilon_H \frac{dt}{dy}$

distribution and the assumed ratio, σ, are discussed in Chapter III. In Chapter IV the effects of surface roughness and axial conduction are discussed. Temperature profiles and the predicted Nusselt numbers are compared to the experimental values and to the theoretical predictions of Martinelli for constant heat flux and to the theoretical predictions of Hefner (16) for constant wall-temperature.

CHAPTER II

MATHEMATICAL DEVELOPMENT

For a fluid flowing turbulently in a cylindrical tube, sufficiently far removed from the extremities of the section to insure absence of end effects, the Reynolds equations reduce to

$$\frac{g_c}{\rho}\frac{\partial \bar{p}}{\partial x} = -\frac{1}{r}\frac{\partial}{\partial r}\left(\overline{rv'u'}\right) + \frac{1}{r}\frac{\partial}{\partial r}\left(\nu\, r\frac{\partial \bar{u}}{\partial r}\right) \tag{4}$$

for the following postulates:

(a) Steady state

(b) Imcompressible flow

(c) Mean motion in the x-direction, the x-axis coinciding with the center line of the tube

(d) Symmetry about the x-axis

(e) Physical properties independent of temperature

Since,

$$\frac{1}{\rho}\frac{d\bar{p}}{dx} = -\frac{2}{R}\frac{\tau_w}{\rho} \tag{5}$$

and

$$\frac{\tau_w}{R} = \frac{\tau}{r} \tag{6}$$

Equation 4 becomes

$$g_c \frac{\tau}{\rho} = \overline{u'v'} - \nu \frac{d\bar{u}}{dr} \tag{7}$$

The energy equation reduces to

$$\bar{u} \frac{\partial \bar{t}}{\partial x} = -\frac{1}{r} \frac{\partial}{\partial r} (r \overline{v't'}) + \frac{1}{r} \frac{\partial}{\partial r} (r \alpha \frac{\partial \bar{t}}{\partial r}) \tag{8}$$

contingent on the following additional postulates:

(f) Negligible dissipative effects

(g) Negligible molecular and eddy transfer of heat in the x-direction.

A heat balance on an annulus of fluid of radius r yields

$$\bar{u} (\frac{\partial \bar{t}}{\partial x}) = \frac{1}{2\pi r \Delta x \rho C_p} (\frac{\partial q}{\partial r}) \tag{9}$$

Hence, Equation 8 can be written as

$$\frac{1}{2\pi r \Delta x \rho C_p} \frac{\partial q}{\partial r} = -\frac{1}{r} \frac{\partial}{\partial r} (r \overline{v't'}) + \frac{1}{r} \frac{\partial}{\partial r} (r \alpha \frac{\partial \bar{t}}{\partial r}) \tag{10}$$

Integration yields

$$\frac{q}{A_r \rho C_p} = -\overline{v't'} + \alpha \frac{\partial \bar{t}}{\partial r} \tag{11}$$

where $A_r = 2\pi r \Delta x$.

If the mean values $\overline{u'v'}$ and $\overline{v't'}$ are expressed as $-\varepsilon_M \frac{d\bar{u}}{dr}$ and $-\varepsilon_H \frac{\partial \bar{t}}{\partial r}$

respectively, Equations 7 and 11 can be written as

$$g_c \frac{\tau}{\rho} = -(\nu + \varepsilon_M) \frac{du}{dr} = (\nu + \varepsilon_M) \frac{du}{dy} \qquad *(12)$$

and

$$\frac{q}{A_r \rho C_p} = (\alpha + \varepsilon_H) \frac{\partial t}{\partial r} = (\alpha + \varepsilon_H) \frac{\partial \theta}{\partial y} \qquad (13)$$

For constant heat flux, $\frac{\partial t}{\partial x}$ = constant; therefore, Equation 9 can be integrated to yield

$$q_w = u_m (\pi r_w^2 \Delta x) \rho C_p (\frac{\partial t}{\partial x}) \qquad (14)$$

Substitution of Equation 14 into 9 yields

$$\frac{\partial q}{\partial r} = q_w \frac{u}{u_m} \frac{2r}{r_w^2} \qquad (15)$$

As an approximation let $u = u_m$ for all r. Then,

$$\frac{q}{A_r} = \frac{q_w}{A_w} \frac{r}{r_w} = \frac{q_w}{A_w} (1 - \frac{y}{R}) \qquad (16)$$

The heat-transfer coefficient for the system as discussed can be defined as

$$q_w = hA_w (t_w - t_m) = hA_w \theta_m \qquad (17)$$

---

*Hereafter, all mean valued quantities will be written without the bar.

Therefore, the Nusselt number can be expressed as

$$Nu = \frac{hD}{k} = \frac{q_w D}{A_w k \Theta_m} = T^* \frac{Pr Re \lambda}{\Theta_m} \tag{18}$$

where

$$\Theta_m = \frac{\int_0^R \Theta\, u\, r\, dr}{\int_0^R u\, r\, dr} = \frac{2}{u_m R^2} \int_0^R \Theta\, u\, r\, dr \tag{19}$$

To facilitate the development of an expression for the temperature, Θ, the flow regime is divided into three regions and discussed accordingly.

Laminar Layer.--In the laminar layer ε_M and ε_H are postulated to be negligible. In addition, the shear and the heat-transfer rate are assumed to be constant. Equation 13 for $0 \leq y^+ \leq y_1^+$, becomes

$$\int_0^{\Theta} d\Theta = T^* Pr \int_0^{y^+} d\beta \tag{20}$$

Hence,

$$\Theta = T^* Pr\, y^+ \tag{21}$$

Buffer Layer.--In the buffer layer ε_M and ε_H are considered to be of comparable magnitude to ν and α . The shear and the heat-transfer rate

are to be constant for $y^+ \leq 30$ and are linear thereafter. The boundary limit, y_T^+, between the buffer layer and turbulent core is determined from the existing experimental data as discussed in the introduction and in Chapter IV. Equation 13 for $y_1^+ \leq y^+ \leq y_2^+$, becomes

$$\int_{\theta_1}^{\theta} d\theta = T^* \int_{y_1^+}^{y^+} \frac{\nu \, d\xi}{\alpha + \varepsilon_H} \tag{22}$$

From equation 12

$$(\nu + \varepsilon_M) = \frac{\frac{g_c \frac{\tau_w}{\rho}}{\frac{du}{dy}}}{} = \frac{\nu}{\frac{du^+}{dy^+}} \tag{23}$$

Since $u^+ = C_1 + C_2 \ln y^+$ in the region $y_1^+ \leq y^+ \leq y_2^+$, then

$$(\nu + \varepsilon_M) = \frac{\nu \, y^+}{C_2} \tag{24}$$

Therefore,

$$\varepsilon_H = \sigma \varepsilon_M = \sigma \left(\frac{\nu y^+}{C_2} - \nu \right) \tag{25}$$

Substitution into equation 22 yields

$$\int_{\theta_1}^{\theta} d\theta = \frac{T^*}{\sigma} \int_{y_1^+}^{y^+} \frac{d\xi}{\frac{1}{\sigma \, Pr} - 1 + \frac{\xi}{C_2}} \tag{26}$$

Hence,

$$\theta = \frac{T^*}{\sigma}\left(y_1^+ \sigma \, Pr + C_2 \ln \frac{C_2\left(\frac{1}{\sigma \, Pr} - 1\right) + y^+}{C_2\left(\frac{1}{\sigma \, Pr} - 1\right) + y_1^+} \right) \tag{27}$$

Equation 13 for $y_2^+ \leq y^+ \leq y_T^+$, becomes

$$\int_{\theta_2}^{\theta} d\theta = T^* \int_{y_2^+}^{y^+} \frac{\nu \left(1 - \frac{\eta}{R^+}\right)}{\alpha + \varepsilon_H} \, d\eta \tag{28}$$

Since $u^+ = C_3 + C_4 \ln y^+$ in the region $y_2^+ \leq y^+ \leq y_T^+$, then

$$(\nu + \varepsilon_M) = \frac{\nu y^+}{C_4}\left(1 - \frac{y^+}{R^+}\right) \tag{29}$$

Therefore

$$\varepsilon_H = \sigma \varepsilon_M = \sigma\left(\frac{\nu y}{C_4}\left(1 - \frac{y^+}{R^+}\right) - \nu\right) \tag{30}$$

Substitution into Equation 28 yields

$$\int_{\theta_2}^{\theta} d\theta = \frac{T^*}{\sigma} \int_{y_2^+}^{y^+} \frac{\left(1 - \frac{\eta}{R^+}\right)}{\frac{1}{\sigma \, Pr} - 1 + \frac{\eta}{C_4}\left(1 - \frac{\eta}{R^+}\right)} \, d\eta \tag{31}$$

Hence,

$$\Theta = \frac{T^*}{\sigma}\left\{ y_1^+ \sigma \, Pr + C_2 \ln \frac{C_2\left(\frac{1}{\sigma\, Pr} - 1\right) + y_2^+}{C_2\left(\frac{1}{\sigma\, Pr} - 1\right) + y_1^+} + \right. \tag{32}$$

$$\frac{C_4}{2}\left(1 - \frac{1}{\sqrt{1 + \frac{4C_4 M}{R^+}}}\right) \ln \frac{y^+ - \frac{R^+}{2}\left(1 + \sqrt{1 + \frac{4C_4 M}{R^+}}\right)}{y_2^+ - \frac{R^+}{2}\left(1 + \sqrt{1 + \frac{4C_4 M}{R^+}}\right)} +$$

$$\left. \frac{C_4}{2}\left(1 + \frac{1}{\sqrt{1 + \frac{4C_4 M}{R^+}}}\right) \ln \frac{y^+ - \frac{R^+}{2}\left(1 - \sqrt{1 + \frac{4C_4 M}{R^+}}\right)}{y_2^+ - \frac{R^+}{2}\left(1 - \sqrt{1 + \frac{4C_4 M}{R^+}}\right)} \right\}$$

Turbulent Core.—The effective magnitude of α is considered negligible compared to ε_H, and ν has been shown to be negligible compared to ε_M. The shear and heat-transfer rate are linear as stated in Equations 6 and 16 respectively. Equation 13, for $y_T^+ \leq y^+ \leq R$, becomes

$$\int_{\Theta_T}^{\Theta} d\Theta = T^* \int_{y_T^+}^{y^+} \frac{\nu\left(1 - \frac{\beta}{R^+}\right)}{\varepsilon_H} \, d\beta \tag{33}$$

From Equation 12

$$\varepsilon_M = \frac{g_c \frac{\tau_w}{\rho}\left(1 - \frac{y}{R}\right)}{\frac{du}{dy}} = \frac{\nu\left(1 - \frac{y^+}{R^+}\right)}{\frac{du^+}{dy^+}} \tag{34}$$

Since $u^+ = C_3 + C_4 \ln y^+$ in the turbulent core, then

$$\varepsilon_M = \frac{\nu \left(1 - \frac{y^+}{R^+}\right) y^+}{C_4} \tag{35}$$

Therefore,

$$\varepsilon_H = \sigma \varepsilon_M = \sigma \frac{\nu \left(1 - \frac{y^+}{R^+}\right) y^+}{C_4} \tag{36}$$

Substituting into Equation 33 yields

$$\int_{\Theta_T}^{\Theta} d\Theta = T^* \frac{C_4}{\sigma} \int_{y_T^+}^{y^+} \frac{d\xi}{\xi} \tag{37}$$

Hence,

$$\Theta = \frac{T^*}{\sigma} \left\{ y_1^+ \sigma \, Pr + C_2 \ln \frac{C_2 M + y_2^+}{C_2 M + y_1^+} + \right. \tag{38}$$

$$\frac{C_4}{2}\left(1 - \frac{1}{\sqrt{1 + \frac{4C_4 M}{R^+}}}\right) \ln \frac{y_T^+ - \frac{R^+}{2}\left(1 + \sqrt{1 + \frac{4C_4 M}{R^+}}\right)}{y_2^+ - \frac{R^+}{2}\left(1 + \sqrt{1 + \frac{4C_4 M}{R^+}}\right)} +$$

$$\left. \frac{C_4}{2}\left(1 + \frac{1}{\sqrt{1 + \frac{4C_4 M}{R^+}}}\right) \right.$$

$$\ln \frac{y_T^+ - \frac{R^+}{2}\left(1 - \sqrt{1 + \frac{4C_4 M}{R^+}}\right)}{y_2^+ - \frac{R^+}{2}\left(1 - \sqrt{1 + \frac{4C_4 M}{R^+}}\right)} + C_4 \ln \frac{y^+}{y_T^+} \Bigg\}$$

The mean temperature can be calculated from the temperature distributions as given in Equations 21, 27, 32 and 38. That is

$$\Theta_m = \frac{2}{u_m R^2} \int_0^R \Theta\, u\, (R - y)\, dy \tag{16b}$$

which can be rearranged to yield

$$\Theta_m = \frac{8}{Re^2 \lambda} \int_0^{R^+} \Theta\, u^+ (R^+ - y^+)\, dy^+ \tag{16c}$$

To evaluate the Nusselt number, Equations 18 and 16c are combined to yield

$$\frac{1}{Nu} = \frac{8}{T^* Pr\, Re^2 \lambda} \int_0^{R^+} \Theta\, u^+ (R^+ - y^+)\, dy^+ \tag{39}$$

Substitution of the appropriate temperature and velocity distributions into Equation 39 gives

$$\frac{1}{Nu} = \frac{8}{Pr' Re^3 \lambda^2} \left\{ Pr' \int_0^{y_1^+} (R^+ - y^+)(y^+)^2 dy^+ + \right. \tag{40}$$

$$\int_{y_1^+}^{y_2^+} \left(y_1^+ Pr' + C_2 \ln \frac{C_2 M + y^+}{C_2 M + y_1} \right) (C_1 + C_2 \ln y^+)\,(R - y^+)\, dy^+ +$$

$$\int_{y_2^+}^{y_T^+} \left[y_1^+ Pr' + C_2 \ln \frac{C_2 M + y_2^+}{C_2 M + y_1^+} + \frac{C_4}{2} \left(1 - \frac{1}{\sqrt{1 + \frac{4 C_4 M}{R^+}}} \right) \right.$$

$$\ln \frac{y^+ - \frac{R^+}{2}\left(1 + \sqrt{1 + \frac{4C_4 M}{R^+}}\right)}{y_2^+ - \frac{R^+}{2}\left(1 + \sqrt{1 + \frac{4C_4 M}{R^+}}\right)} + \frac{C_4}{2}\left(1 + \frac{1}{\sqrt{1 + \frac{4C_4 M}{R^+}}}\right)$$

$$\left. \ln \frac{y^+ - \frac{R^+}{2}\left(1 - \sqrt{1 + \frac{4C_4 M}{R^+}}\right)}{y_2^+ - \frac{R^+}{2}\left(1 - \sqrt{1 + \frac{4C_4 M}{R^+}}\right)} \right] (C_3 + C_4 \ln y^+)\,(R^+ - y^+)\, dy^+ +$$

$$\int_{y_T^+}^{R^+} \left[y_1^+ Pr' + C_2 \ln \frac{C_2 M + y_2^+}{C_2 M + y_1^+} + \frac{C_4}{2} \left(1 - \frac{1}{\sqrt{1 + \frac{4C_4 M}{R^+}}} \right) \right.$$

$$\ln \frac{y_T^+ - \frac{R}{2}\left(1 + \sqrt{1 + \frac{4C_4 M}{R^+}}\right)}{y_2^+ - \frac{R}{2}\left(1 + \sqrt{1 + \frac{4C_4 M}{R^+}}\right)} + \frac{C_4}{2}\left(1 + \frac{1}{\sqrt{1 + \frac{4C_4 M}{R^+}}}\right)$$

$$\left. \left. \ln \frac{y_T^+ - \frac{R^+}{2}\left(1 - \sqrt{1 + \frac{4C_4 M}{R^+}}\right)}{y_2^+ - \frac{R^+}{2}\left(1 - \sqrt{1 + \frac{4C_4 M}{R^+}}\right)} + C_4 \ln \frac{y^+}{y_T^+} \right] (C_3 + C_4 \ln y^+)(R^+ - y^+) dy^+ \right\}$$

This equation was solved by utilizing a Remington Rand Model ERA 1101 digital computer. An analytic expression was used for the laminar layer. The trapezodial rule was employed for the buffer layer and turbulent core, with forty-five and thirty intervals respectively. A difference of less than one per cent was obtained when the number of intervals was increased from thirty for the buffer layer and twenty for the turbulent core to the above number for Pr = 0.02 and Re = 10^6.

CHAPTER III

EFFECTS OF THE VELOCITY DISTRIBUTIONS AND THE RATIO OF THE EDDIES

Solution of the energy equation embodying the assumptions as listed in Chapter II is contingent upon the knowledge of the velocity distribution and the expression $(\alpha + \varepsilon_H)$, which in turn is dependent on the ratio, σ, and the velocity gradient.

The utility of the dimensionless universal velocity distribution has partially compensated for the lack of exactness. Recent critical reviews of the distribution are presented by Ross (17), Ruth and Yang (18) and Rothfus, et al., (19). Brooks and Berggren (20) contend that the peculiar S-shaped velocity gradient as presented by Nikuradse and others is in error. They state, "the proper fitting of an empirical velocity profile curve to the almost-equal velocities near the center should be such that the successive derivatives of the profile give smooth and logical curves across the line of maximum velocity." It was pointed out that the S-shape is required to avoid a peaked mixing length in the central region.

From Equation 12 it can be understood why small errors in the velocity distribution may cause large errors in ε_M and hence ε_H. Table 2 compares the velocity gradients which were determined graphically by Nikuradse (21) with the velocity gradients obtained from the

Table 2. Comparison of Velocity Gradients

	Re = 43.4×10^3 R = 1.0 cm		Re = 396×10^3 R = 2.5 cm		Re = 1959×10^3 R = 5.0 cm		Re = 3240×10^3 R = 5.0 cm	
$\frac{y}{R}$	$\left(\frac{du}{dy}\right)_{graph}$	$\left(\frac{du}{dy}\right)_{law}$	$\left(\frac{du}{dy}\right)_{graph}$	$\left(\frac{du}{dy}\right)_{law}$	$\left(\frac{du}{dy}\right)_{graph}$	$\left(\frac{du}{dy}\right)_{law}$	$\left(\frac{du}{dy}\right)_{graph}$	$\left(\frac{du}{dy}\right)_{law}$
0.02	1348	3360	1370	3040	1890	3880	2080	2080
0.04	693	840	704	760	977	969	1085	1040
0.07	411	480	416	434	575	554	645	594
0.10	302	336	304	304	414	388	466	416
0.15	220	224	215	203	288	258	319	277
0.20	181	168	169	152	223	194	246	208
0.30	129	112	123	101	157	129	168	139
0.40	99	84.0	92.5	76.0	118	96.9	128	104
0.50	81	67.2	76	60.8	98	77.5	104	83.1
0.60	68	56.0	62	50.7	81	64.6	86.7	69.3
0.70	55	48.0	51.7	43.4	65.6	55.4	69.5	59.4
0.80	44	42.0	41.0	38.0	52.0	48.4	55.7	51.9
0.90	30	37.3	27.8	33.8	35.6	43.1	38.8	46.2
0.96	18.5	35.0	17.5	31.7	22.3	40.4	23.7	43.3
0.98	13.0	34.3	12.3	31.0	15.9	39.5	16.8	42.4
1.00		33.6		30.4		38.8		41.6

$\left(\frac{du}{dy}\right)_{graph}$ = graphically determined by Nikuradse

$\left(\frac{du}{dy}\right)_{law}$ = universal velocity distribution

universal velocity distribution. The largest deviations are found in the regions adjacent to the wall and near the center of the pipe. It should be noted that Nikuradse listed a finite velocity at the wall, from which his gradients were obtained. If the velocity gradients obtained from the universal velocity distribution are substituted for Nikuradse's graphically determined gradients in Lyon's calculation for Re = 43,400, the difference in the calculated values for the Nusselt number as shown in Table 3 is small. However, for large Reynolds numbers, this difference apparently is increased. Table 4 shows the calculated Nusselt numbers for Re = 3.24×10^6. The comparison is not conclusive as the Nusselt numbers as listed by Lyon are not indicative of the number of intervals employed in his calculations.

Table 5 compares the velocity gradients for $y^+ = 60$ obtained from the universal velocity distribution with those determined from a modified form of the van Driest velocity distribution. In Appendix II the modification to the latter velocity distribution is shown. In addition, the necessary equations to predict the Nusselt number employing this velocity distribution are developed. The flow field was divided into two regions as follows: Laminar-Buffer layer - $(0 \leq y^+ \leq 60)$; in this region both the molecular and eddy terms are considered. The shear and the heat-transfer rate are linear. Turbulent core - $(60 \leq y^+)$; the effective magnitude of α is considered to be negligible. The shear and heat-transfer rate are linear. The division at $y^+ = 60$ rather than $y^+ = 70$ was selected for convenience. Table 6 compares Nusselt numbers

Table 3. Calculation Sheet for Re = 43,400. (Table V-b-Lyon) The columns shown have been re-evaluated using the velocity gradient calculated from the dimensionless universal velocity distribution.

S	$\frac{\varepsilon_M}{\nu} + 1$	$\left[\int_0^q VSdS\right]^2$	$\frac{k}{SK}$ for Pr.	
		0.1	0.01	
No. 1	No. 6	No. 7	No. 8	
1.00	1	0.2522	0.2522	
0.98	4.427	0.1828	0.2377	
0.96	17.34	0.0896	0.2029	
0.93	29.41	0.0574	0.1716	
0.90	40.66	0.0411	0.1461	
0.85	57.60	0.0267	0.1134	
0.80	72.29	0.0187	0.0889	
0.70	94.87	0.0103	0.0551	
0.60	108.4	0.0059	0.0337	
0.50	112.9	0.0034	0.0197	
0.40	108.4	0.0019	0.0106	
0.30	94.87	0.0009	0.0048	
0.20	72.29	0.0003	0.0016	
0.10	40.66	0.0001	0.0003	
0.04	17.34			
0.02	8.857			
0				
	Nu	30.1	10.4	
	Nu (Lyon)	30.5	10.3	

Table 4. Calculation Sheet for Re = 3.24×10^6. (Table V-d-Lyon) The columns shown have been re-evaluated using the velocity gradient calculated from the dimensionless universal velocity distribution.

S	$\frac{\varepsilon_M}{\nu} + 1$	$\left[\int_0^q VSdS\right]^2 \frac{k}{SK}$ for Pr.	
		0.1	0.01
No. 1	No. 6	No. 7	No. 8
1.00	1	0.2505	0.2505
0.999	22.14	0.08032	
0.998	44.23	0.04691	
0.997	66.28	0.03312	
0.996	88.29	0.02558	
0.995	90.35	0.02133	0.1312
0.99	193.8	0.01214	0.08409
0.985	274.1	0.008617	0.06539
0.98	434.3	0.005445	0.04527
0.97	644.9	0.003610	0.03173
0.96	850.9	0.002684	0.02432
0.93	1443.	0.001476	0.01389
0.90	1994.	0.000986	0.009434
0.85	2825.	0.000602	0.005830
0.80	3546.	0.000408	0.003981
0.70	4654.	0.000215	0.002112
0.60	5318.	0.000122	0.001200
0.50	5540.	0.000069	0.000683
0.40	5318.	0.000038	0.000369
0.30	4654.	0.000018	0.000181
0.20	3546.	0.000007	0.000071
0.10	1994.	0.000002	0.000014
	Nu	654	104
	Nu (Lyon)	613.4	100

Table 5. Comparison of Velocity Gradients

	Re = 10^4		Re = 10^5	
y^+	$\left(\frac{du^+}{dy^+}\right)$ van D.	$\left(\frac{du^+}{dy^+}\right)$ law	$\left(\frac{du^+}{dy^+}\right)$ van D.	$\left(\frac{du^+}{dy^+}\right)$ law
2.5	0.985	1.0	0.991	1.0
5	0.893	1.0	0.905	1.0
10	0.533	0.50	0.543	0.50
20	0.204	0.25	0.211	0.25
30	0.111	0.167	0.116	0.167
40	0.0724	0.125	0.0770	0.125
50	0.05270	0.100	0.570	0.100
60	0.0410	0.082	0.0451	0.082

Subscripts: van D. - modified van Driest velocity distribution law - universal velocity distribution

Table 6. Comparison of Nusselt Numbers Based on the Universal Velocity Distribution and the Modified van Driest Velocity Distribution

Pr	Re x 10^{-3}	Pe x 10^{-2}	Nu van D.	Nu
0.02	10	2	5.25	5.30
1	10	100	38.4	38.3
10	10	1,000	103.	88.1
100	10	10,000	208.	119.
0.02	100	20	13.7	13.7
1	100	1,000	222.	220.
10	100	10,000	704.	612.
100	100	100,000	1530.	879.

Subscript: van D - van Driest

calculated in this manner with those obtained using the universal velocity distribution throughout the field of flow.

For Pr = 0.02 the two velocity distributions yield essentially the same Nusselt number. The remaining calculated values indicate that the role of the velocity distribution near the wall becomes more important with increasing Prandtl numbers. The improvement obtained for large Prandtl numbers when the van Driest velocity distribution is employed is shown in Figure 5, which utilizes a comparison made by Rannie in his thesis between his theoretical predictions and experimental data.

In calculations for fluids of small Prandtl numbers the region adjacent to the wall contributes only a small part of the total calculated value of the Nusselt number. This situation is reversed for ordinary fluids. For these fluids it is extremely important to have an accurate velocity distribution in the proximity of the wall. For ordinary fluids the more accurate velocity distribution proposed by van Driest affords better agreement between the predicted heat-transfer coefficient and the experimental data.

The ratios of the eddy diffusivities, $\sigma \equiv \varepsilon_H/\varepsilon_M$, has been described as the "true measure of our ignorance of the mechanism of heat transfer in turbulent motion." (22) Reichardt (14) postulates that $1 \leq \sigma \leq 2$. Jenkins (23) proposed a modification to Prandtl's mixing length theory to account for the loss of heat and momentum during the time the eddy is displaced. For Prandtl numbers less than one, his theory predicts that the ratio of the eddy diffusivities will be less

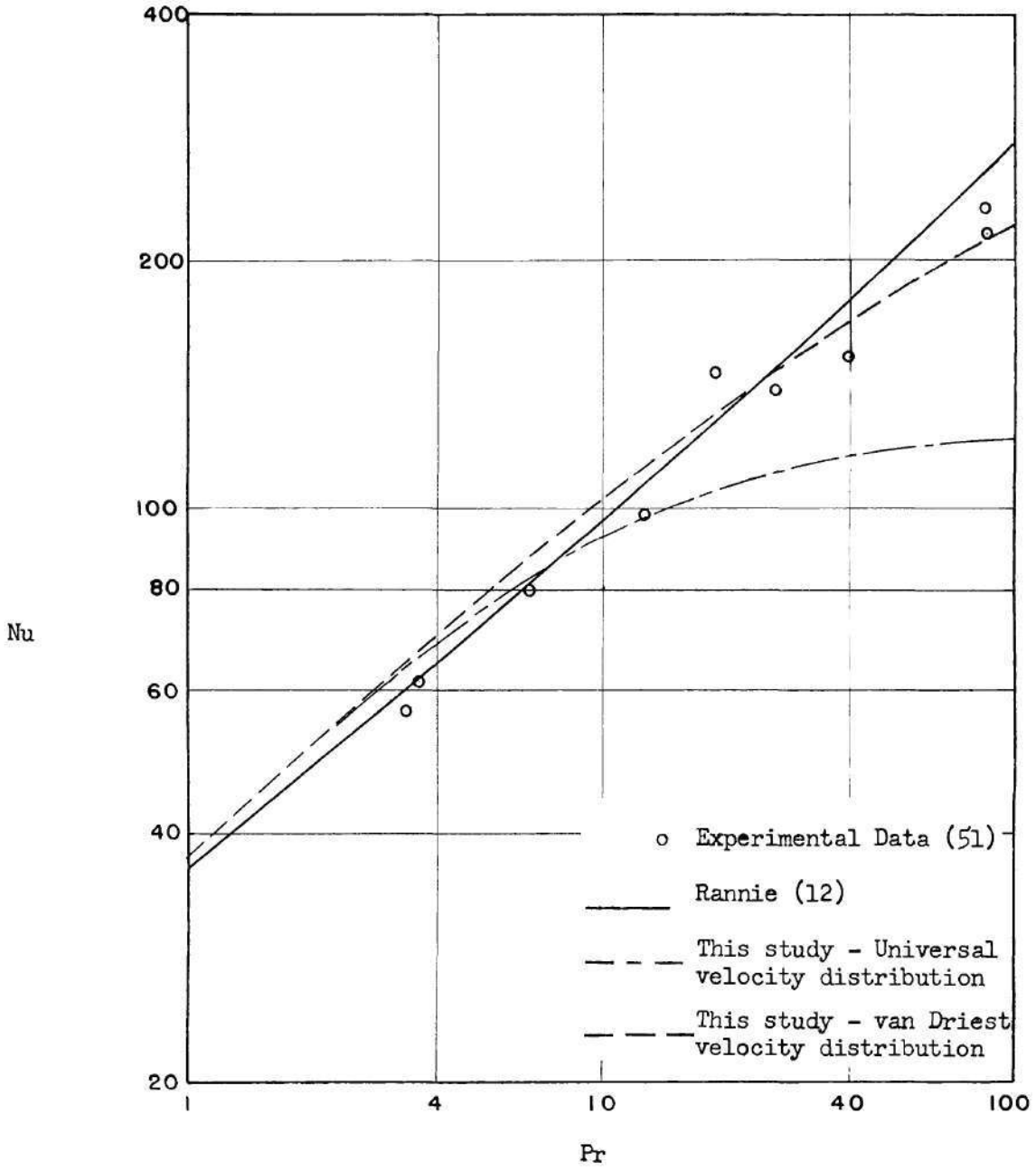

Figure 5. Predicted and Experimental Nusselt Numbers at Large Prandtl Number.

than one. The extensive studies of air conducted by Sage, et al., (24), (25) and (26) indicate that the ratio is greater than one. Isakoff and Drew (27) and Brown, Amstead and Short (28) have measured velocity and temperature distributions for mercury flowing in pipes and have calculated the ratios of the eddy diffusivities from their results. Isakoff and Drew report values ranging up to approximately $\sigma = 1.7$. Since the fluid temperature did not extrapolate well to the wall-temperature, their observations must be regarded with caution. Brown, et al., report values ranging up to approximately $\sigma = 0.95$. Unfortunately, the spacing of their data does not satisfactorily facilitate a numerical analysis of the temperature gradient. If either graphical or least squares methods are employed, somewhat higher values may be obtained for the eddy diffusivity of heat and consequently higher values for the ratio of the eddy diffusivities result.

Sleicher (29), using a mathematical approach proposed by Tribus and Klein (30) to solve the energy equation for arbitrary temperature distribution, adjusted the predicted ratio of eddy diffusivities as proposed by Jenkins to correspond to his measured ratio for air. Using this adjusted ratio and a smoothed velocity distribution - Deissler (10), Reichardt (13), Laufer - Re = 50,000 (31), and Sleicher - he obtained Nusselt numbers in good agreement with the data. The Martinelli model, employing the velocity distributions of either Nikuradse, Deissler, or Laufer in the dimensionless

form, will yield Nusselt numbers comparable to these results only if the ratio, σ, is sufficiently small. A typical case is illustrated in Table 7 for Re = 10^5 and Pr = 0.02. The values for ε_H/ν were obtained from Sleicher and the values for ε_M/ν were calculated from the above respective velocity distributions. For these velocity distributions, the resulting ratio of the eddies required to bring the theory into agreement with the data is inconsistent with our limited knowledge of this parameter. In this analysis the ratio, σ, was included in the mathematical development, although for the final numerical computations a value equal to unity was utilized. The results may easily be re-evaluated for a mean value of the ratio different from unity.

Table 7. Ratios, Based on Sleicher's Computations, Required for Martinelli's Theory to Agree with Experimental Data

$Re = 10^5$, $Pr = 0.02$

$\frac{r}{r_w}$	$\frac{\left(\frac{\varepsilon_H}{\nu}\right)_S}{\left(\frac{\varepsilon_M}{\nu}\right)_{law}}$	$\frac{\left(\frac{\varepsilon_H}{\nu}\right)_S}{\left(\frac{\varepsilon_M}{\nu}\right)_D}$	$\frac{\left(\frac{\varepsilon_H}{\nu}\right)_S}{\left(\frac{\varepsilon_M}{\nu}\right)_L}$
0.1	1.02	1.13	1.19
0.2	0.574	0.636	0.667
0.3	0.437	0.486	0.508
0.4	0.383	0.426	0.445
0.5	0.367	0.408	0.427
0.6	0.387	0.430	0.450
0.7	0.402	0.447	0.467
0.75	0.372	0.413	0.433
0.8	0.369	0.410	0.429
0.85	0.352	0.391	0.409
0.9	0.311	0.346	0.362
Nu	12.4	12.2	9.61

Subscripts: S-Sleicher; law-Nikuradse; D-Deissler; L-Laufer

CHAPTER IV

DISCUSSION OF RESULTS

An excellent review of the experimental investigations has been presented by Lubarsky and Kaufman (32). Subsequent investigations have been conducted by Chelemer (33); Mikheyev, Baum, Voskerensky , and Fedynsky (34); Hall and Crofts (35); Kuczen and Bump (36); Brown, Amstead and Short (28); and Seban and Casey (37). Their results are in agreement with the bulk of the data as reviewed by Lubarsky and Kaufman, except for the work of Brown, et al., which is higher. Figure 1 presents the data, excluding those investigations which overlap the region as shown. The data for mercury have been re-evaluated using the thermal conductivity data of Ewing, Seebold, Grand and Miller (38).

Because the results are lower than the theoretical predictions of Martinelli, a continual search has been made to account for an inherent error in the experimental investigations. MacDonald and Quittenton (39) discuss the effect of "wetting" and gas entrainment and conclude that gas entrainment may possibly account for the discrepancy. Hoffman, Chelemer, Stansbury and Boarts (40) conclude that the data are low due to the effect of gas entrainment.

Martinelli and Lyon based their calculations on a smooth surface; yet the experimental investigations were conducted in the presence of

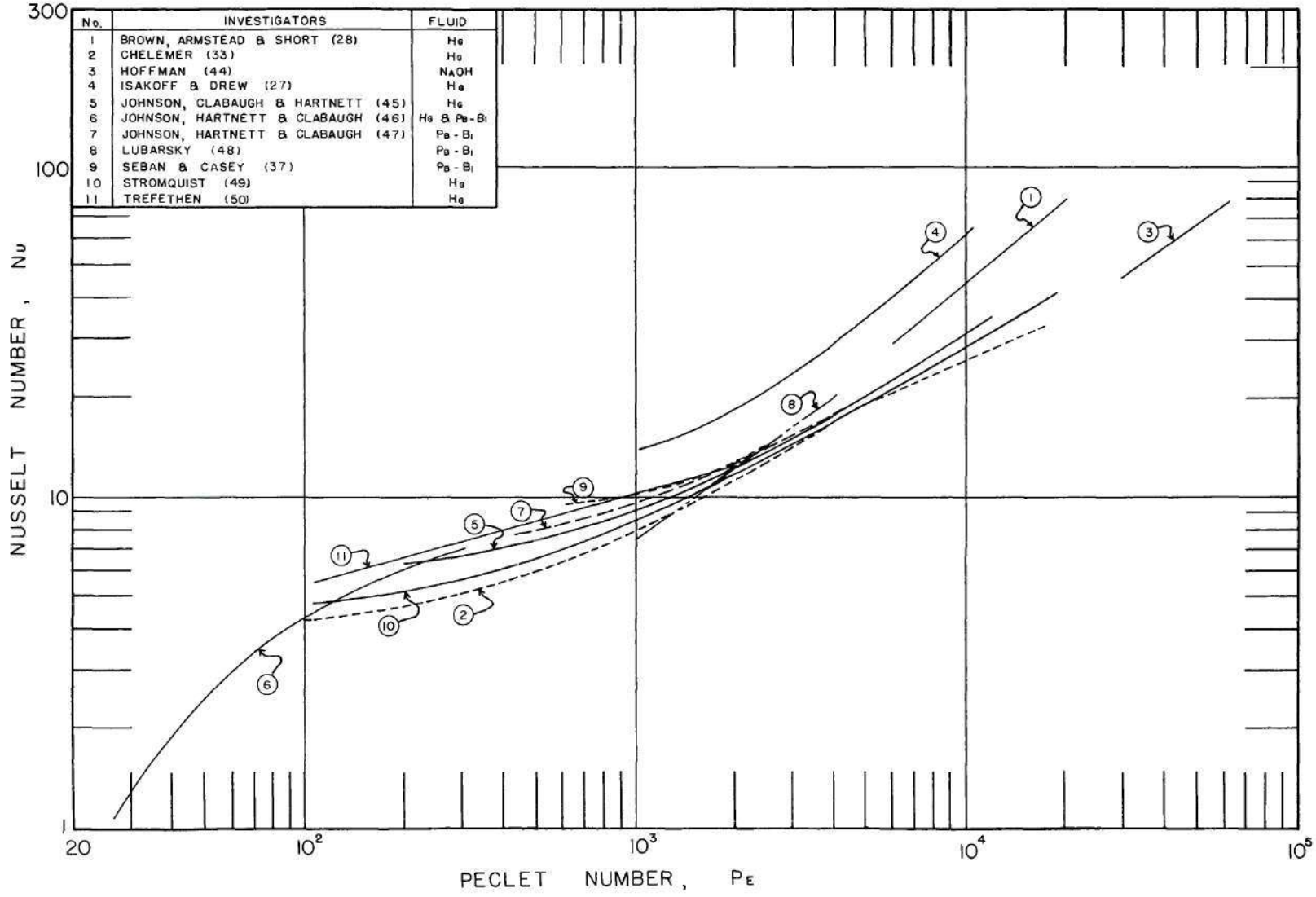

FIGURE 1. EXPERIMENTAL DATA

rough surfaces. Examination of Nikuradse's (41) data for rough pipe indicates that the constants C_3 and C_4 in the velocity distribution decrease with increasing roughness. In addition, the intercept of the curves, which defines the velocity distribution in the buffer layer and turbulent core, is altered. If the velocity data of Brown, et al., are assumed to be representative, values for the constants and intercept obtained from their data can be utilized to ascertain the effect of surface roughness. Employing these adjusted equations, it was found that the theory would predict a six to twelve per cent increase in the heat-transfer coefficient for Pr = 0.01 as shown in Table 8. This effect increases the discrepancy between Martinelli's theory and the experimental data.

Another explanation of the discrepancy between Martinelli's theory and the data may be the model employed. The thermal diffusivity, as postulated in this investigation, is so interrelated in the turbulent core that thermal and eddy diffusivities are not strictly additive. The crude step-like functions employed by this investigation, (Table I), for the diffusivities of heat and momentum leave much to be desired. However, by utilizing this concept and the arbitrary choice of the buffer-layer limit, good agreement is obtained between these predictions and the data for liquid metals. In addition, improved agreement is obtained for normal fluids when the more accurate velocity distribution of van Driest is employed. The choice of the buffer-layer limit, $y_T^+ = 70$, is only approximate. Additional knowledge of the ratio of the eddies

Table 8. Effect of Velocity Distributions and Surface Roughness on Predicted Nusselt Numbers - Martinelli's Model

Pr	Re x 10^{-3}	Nu			
		a	b	c	Smooth
0.01	5	7.26	5.98	7.89	7.41
0.01	10	7.75	6.57	9.05	8.14
0.01	30	9.29	7.99	11.3	10.1
0.01	100	13.4	11.6	16.6	14.9
0.01	300	22.2	19.2	27.9	24.9
0.01	1000	44.3	38.6	56.6	50.3

a - based on Deissler's velocity distribution, $u^+ = 3.8 + 2.78 \ln y^+$
b - based on Laufer's velocity distribution, $u^+ = 5.5 + 2.907 \ln y^+$
c - simulated roughness encountered by Brown, et al. - relative roughness, $\varepsilon/D = 0.00015$

as a function of the radius, Reynolds number and Prandtl number and the extent to which the data for liquid metals are lowered by entrainment of gas must be determined before the lower limit of the turbulent core is known accurately.

A point to note is that at low values of Peclet numbers, values of experimental Nusselt numbers are lower than the theoretical limiting values for constant heat flux and constant wall-temperature. The theoretical or "exact" solutions have neglected molecular and eddy transfer of heat in the axial direction; which for a fluid such as air may be quite valid. However, the validity of these assumptions to obtain an "exact" solution applied to heat transfer in liquid metals is questionable. Trefethen (42) presents an analysis of the situation and concludes that the experimental data appear to demonstrate axial conduction, but in an inconclusive fashion. His correction was applied to the predicted values for Pe < 150. The resulting values for low Prandtl number are compared in Figure 2 to Martinelli's predictions, (shown uncorrected and corrected); to Hefner's predictions for constant wall-temperature, which are based on the same model as this investigation and to the experimental data. The predictions for large Prandtl numbers are shown in Figure 3. The predicted values are also presented in Figure 4 with the Nusselt number as a function of Reynold's number and Prandtl number as a parameter. Table 9 includes all of the predictions of this investigation based on the universal velocity distribution.

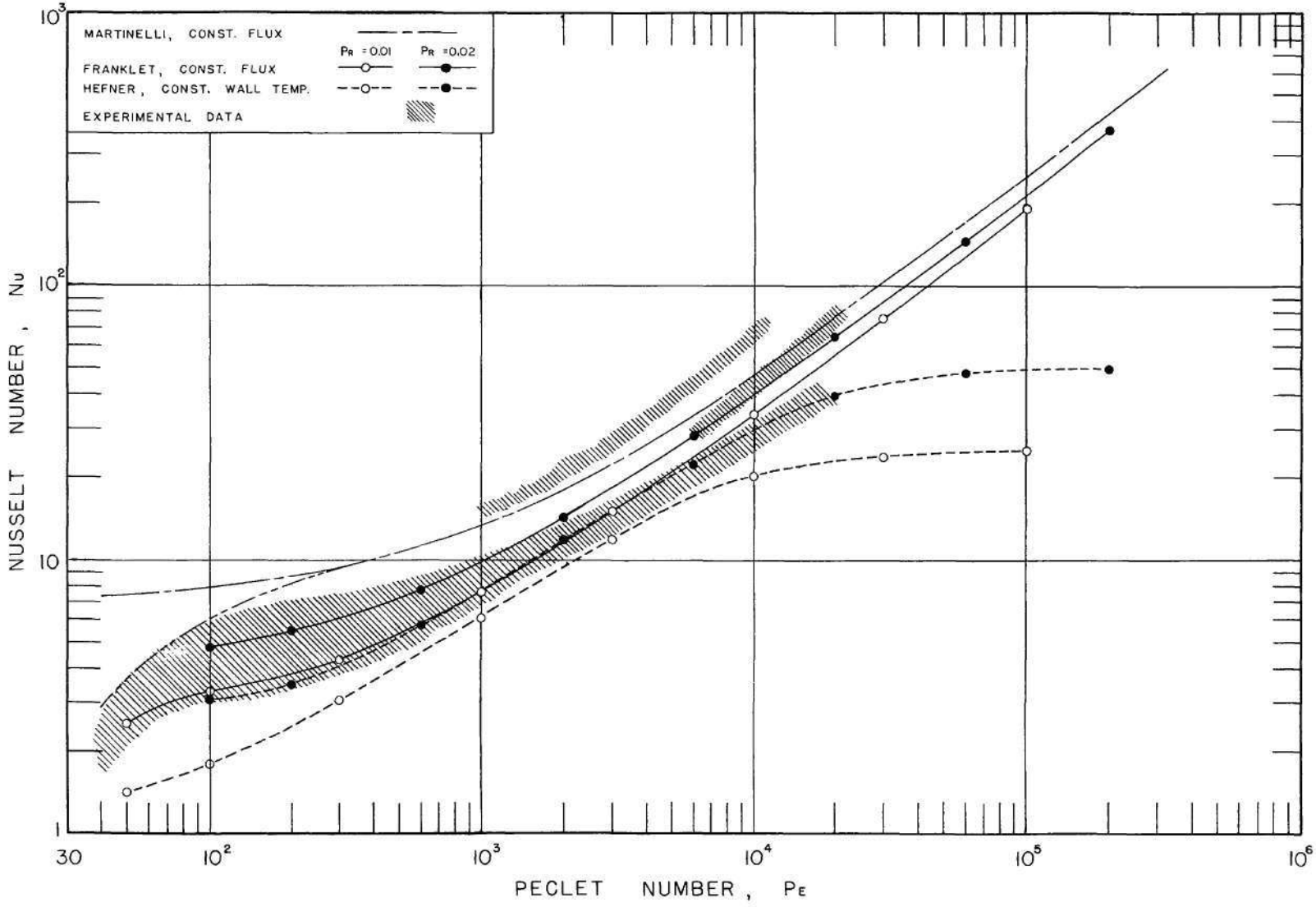

FIGURE 2. NUSSELT NUMBER AS A FUNCTION OF PECLET NUMBER FOR LOW PRANDTL NUMBERS

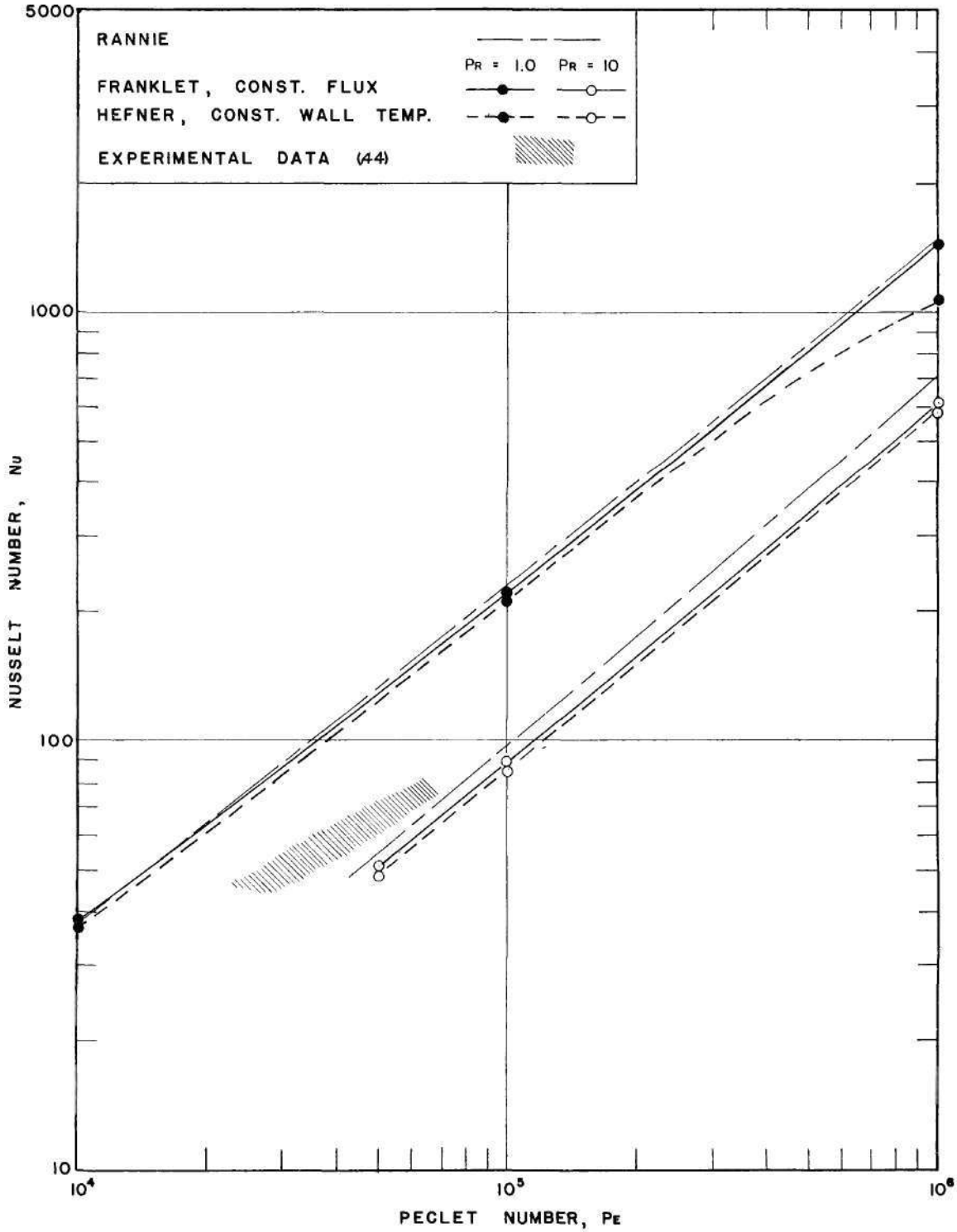

FIGURE 3. NUSSELT NUMBER AS A FUNCTION OF PECLET NUMBER FOR LARGE PRANDTL NUMBERS

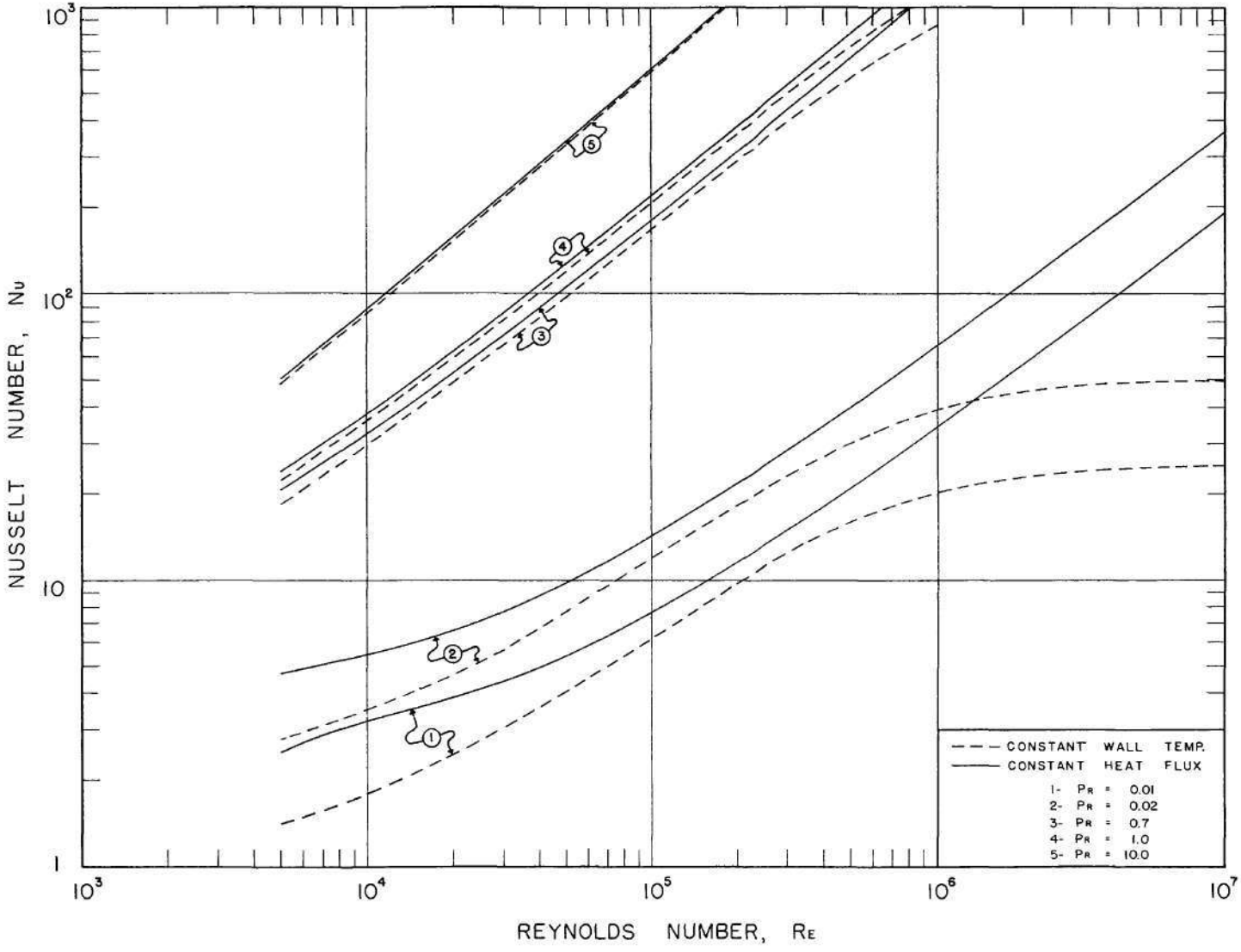

FIGURE 4. NUSSELT NUMBER AS A FUNCTION OF REYNOLDS NUMBER AND PRANDTL NUMBER

Table 9. Predicted Nusselt Numbers Based on the Universal Velocity Distribution

Pr	Re x 10^{-3}	Pe	Nu			
			$y_T^+ = 60$	$y_T^+ = 70$	$y_T^+ = 90$	$y_T^+ = 100$
		Smooth Pipe				
0.005	5	25		2.84	4.25	
0.005	10	50		2.11	2.77	
0.005	30	150		2.40	2.78	
0.005	100	500		4.05	4.45	
0.005	300	1,500		7.75	8.29	
0.005	1,000	5,000			18.4	
0.010	5	50		4.28	5.56	
0.010	10	100		3.62	4.45	
0.010	30	300		4.43	5.00	
0.010	100	1,000		7.72	8.34	
0.010	300	3,000		15.0	15.8	16.2
0.010	1,000	10,000		34.0	35.5	36.1
0.010	3,000	30,000	74.6	76.3	79.0	
0.010	10,000	100,000	189.	193.	198.	
0.015	5	75	4.55	5.20	6.29	
0.015	10	150	4.35	5.12	5.64	
0.015	30	450	5.83	6.21	6.86	
0.015	100	1,500		11.1	11.8	
0.015	300	4,500	21.1	21.7	22.8	
0.015	1,000	15,000	48.6	49.7	51.6	
0.015	3,000	45,000	110.	112.	116.	
0.015	10,000	150,000	280.	284.	292.	
0.020	5	100	5.27	5.86	680.	
0.020	10	200	5.30	5.77	6.58	
0.020	30	600	7.09	7.80	8.49	
0.020	100	2,000	13.7	14.2	15.1	

(Continued)

Table 9. Continued

Pr	Re x 10^{-3}	Pe	Nu			
			$y_T^+ = 60$	$y_T^+ = 70$	$y_T^+ = 90$	$y_T^+ = 100$
		Smooth Pipe				
0.020	300	6,000	27.4	28.2	29.4	
0.020	1,000	20,000	63.6	65.0	67.1	
0.020	3,000	60,000	144.	147.	151.	
0.020	10,000	200,000	368.	374.	382.	
0.025	5	125		6.39	7.20	7.48
0.025	10	250		6.59	7.36	7.67
0.025	30	750		9.25	9.96	10.3
0.025	100	2,500		17.2	18.1	18.4
0.025	300	7,500		34.3	35.6	36.2
0.025	1,000	25,000		79.6	81.9	82.9
0.050	5	250		8.10	8.56	8.71
0.050	10	500		9.59	10.1	10.3
0.050	30	1,500		15.2	15.8	
0.050	100	5,000		30.0	30.9	
0.050	300	15,000		61.9	63.3	
0.050	1,000	50,000		147.	150.	
0.050	3,000	150,000		337.	342.	
0.050	10,000	500,000		870.	881.	
0.70	5	3,500		20.7	20.7	
0.70	10	7,000		32.6	32.7	
0.70	30	21,000		71.7	71.7	
0.70	100	70,000		179.	179.	
0.70	300	210,000		425.	425.	
0.70	1,000	700,000		1,130.	1,130.	
1.00	5	5,000		23.8		
1.00	10	10,000		38.3		
1.00	30	30,000		86.3		

(Continued)

Table 9. Continued

Pr	Re x 10^{-3}	Pe	Nu			
			$y_T^+ = 60$	$y_T^+ = 70$	$y_T^+ = 90$	$y_T^+ = 100$
		Smooth Pipe				
1.00	100	100,000		220.		
1.00	300	300,000		531.		
1.00	1,000	1,000,000		1,430.		
10.0	5	50,000		51.0		
10.0	10	100,000		88.1		
10.0	30	300,000		219.		
10.0	100	1,000,000		612.		
10.0	300	3,000,000		1,590.		
10.0	1,000	10,000,000		4,610.		
100	5	500,000		67.7		
100	10	1,000,000		119.		
100	30	3,000,000		305.		
100	100	10,000,000		879.		
100	300	30,000,000		2,350.		
100	1,000	100,000,000		6,990.		
		Smooth Pipe	$C_3 = 3.8$		$C_4 = 2.78$ (Deissler)	
0.020	30	600		---		
0.020	100	2,000		12.8		
0.020	300	6,000		25.1		
0.020	1,000	20,000		57.3		
0.020	3,000	60,000		128.		
0.020	10,000	200,000		324.		
		Commercial Pipe				
0.020	10	200		5.49		
0.020	30	600		7.49		
0.020	100	2,000		14.3		
0.020	300	6,000		28.0		

(Continued)

Table 9. Continued

Pr	Re x 10^{-3}	Pe	Nu			
			$y_T^+ = 60$	$y_T^+ = 70$	$y_T^+ = 90$	$y_T^+ = 100$
	Rough Pipe	/D = 0.00015	$C_3 = 5.5$	$C_4 = 2.5$		$y_2^+ = 30.$
0.010	300	3,000		14.9	15.7	
0.010	1,000	10,000		33.8	35.2	
0.020	5	100		5.61	6.41	
0.020	10	200		5.69	6.35	
0.020	30	600		7.86	8.53	
0.020	100	2,000		14.0	14.8	
0.020	300	6,000		27.5	28.6	
0.020	1,000	20,000		63.4	65.6	
0.020	3,000	60,000		141.	145.	
0.020	10,000	200,000		356.	363.	
	Rough Pipe	/D = 0.00015	$C_3 = 3.96$	$C_4 = 2.44$		$y_2^+ = 12$
0.010	3,000	30,000		16.5	17.4	
0.010	10,000	100,000		37.4	38.9	
0.020	5	150		6.38	7.27	
0.020	10	200		6.33	7.04	
0.020	30	600		8.89	9.64	
0.020	100	2,000		15.7	16.6	
0.020	300	6,000		30.6	31.8	
0.020	1,000	20,000		70.6	73.0	
0.020	3,000	60,000		156.	160.	
0.020	10,000	200,000		391.	399.	
	Rough Pipe	/D = 0.00015	$C_3 = 6.0$	$C_4 = 2.22$		$y_2^+ = 25.5$
0.010	3,000	30,000		17.9	18.8	

(Continued)

Table 9. Concluded

Pr	Re x 10^{-3}	Pe	Nu			
			$y_T^+ = 60$	$y_T^+ = 70$	$y_T^+ = 90$	$y_T^+ = 100$
	Rough Pipe	/D = 0.00015	$C_3 = 6.0$		$C_4 = 2.22$	$y_2^+ = 25.5$
0.010	10,000	100,000		40.9	42.5	
0.020	5	100		6.33	7.18	
0.020	10	200		6.54	7.27	
0.020	30	600		9.25	10.0	
0.020	100	2,000		16.7	17.6	
0.020	300	6,000		32.9	34.3	
0.020	1,000	20,000		76.5	80.1	
0.020	3,000	60,000		171.	176.	
0.020	10,000	200,000		433.	442.	
	Rough Pipe	/D = 0.00015	$C_3 = 4.76$		$C_4 = 2.44$	$y_2^+ = 18$
0.010	3,000	30,000			16.9	
0.010	10,000	100,000			37.8	
0.020	5	100			—	
0.020	10	200			6.78	
0.020	30	600			9.38	
0.020	100	2,000			16.0	

Since the data of Brown, et al., and the predictions of this investigation do not exactly coincide, it would not be expected that the temperature profiles concisely agree. However, for Pr = 0.0201, Re = 2.5×10^5 and for Pr = 0, Re = 5.65×10^5, the temperature profiles are compared as shown in Figure 6.

Friction factors for smooth and rough pipe were based on the empirical equations of Drew, Koo and McAdams (43), except when attempting to duplicate the surface roughness encountered by Brown, et al., in which case the Moody plot was utilized for a relative roughness, $\varepsilon/D = 0.00015$.

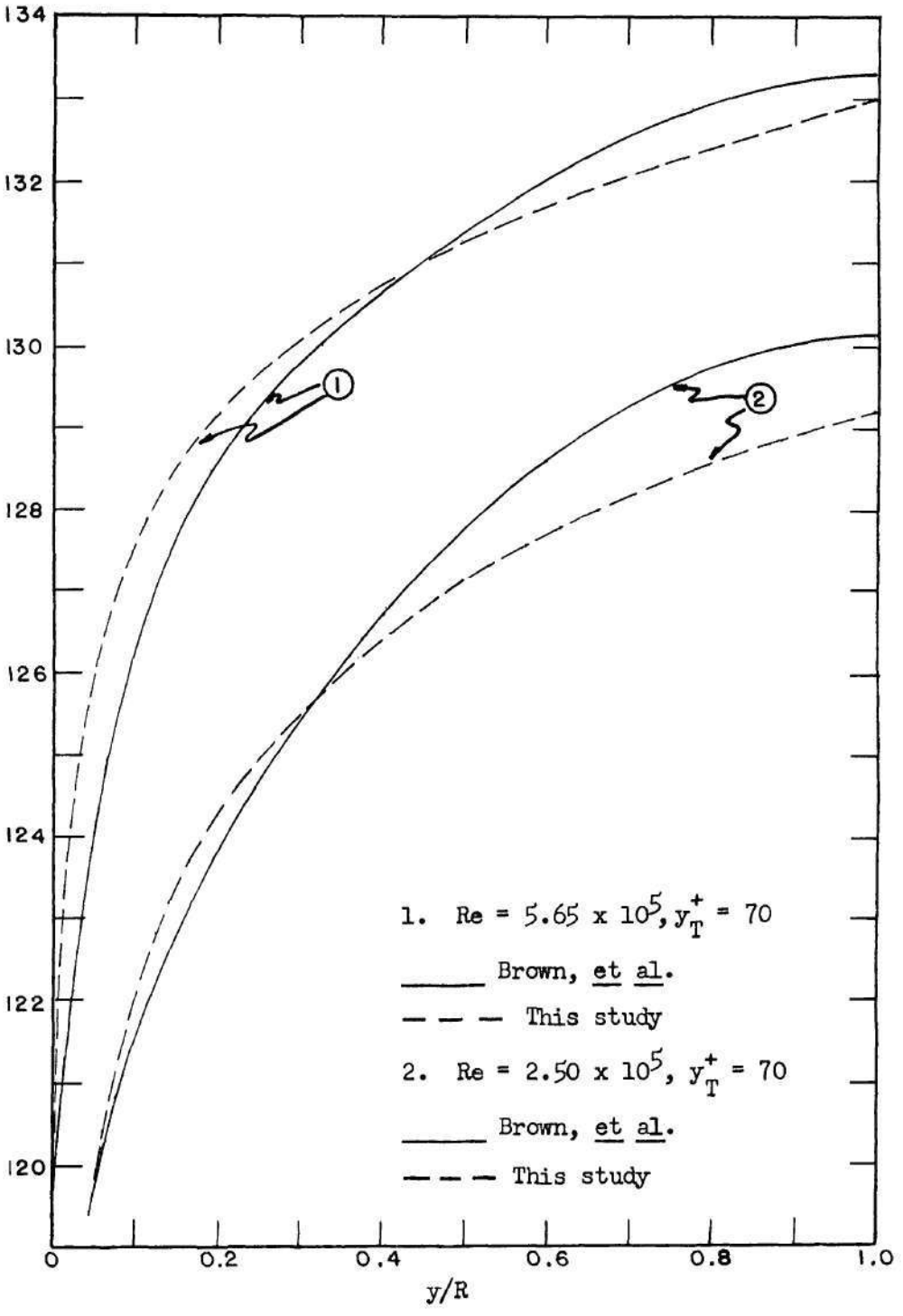

Figure 6. Comparison of Predicted Temperature Distributions with the Experimental Temperature Distributions of Brown, Amstead and Short.

CHAPTER V

CONCLUSIONS AND RECOMMENDATIONS

The discrepancy between Martinelli's theory and the experimental data has not been explained on the basis of experimental error. Perhaps the best explanation proposed is the entrainment of gases. However, to explain the large discrepancy, the geometrical shape of the entrained gas must deviate radically from a spherical form. If the gas is present as extended planes or gaps, minute quantities of gas suffice to explain the differences; yet, for these small quantities of gas the geometrical form postulated is not probable. An extrapolation between these two geometrical shapes should be considered with caution. A combination of gas entrainment and lower values for the ratio of the eddy diffusivities might lessen the distorted geometrical form required to bring the experimental data and Martinelli's theory into agreement. If the data of Brown, Amstead and Short is considered to be representative, the effect of roughness approximately offsets the effect of the lower values of the ratio of diffusivities. Hence, an error in excess of forty per cent is still to be accounted for. To alleviate this difference, the model employed in this study was proposed. The experimental heat-transfer data were used to evaluate the lower limit

of the turbulent core and the region in which the thermal diffusivity is effective. Mindful of these preliminary remarks, the following conclusions may be drawn as a result of this investigation:

1. Good agreement is obtained between the experimental heat-transfer data and the predictions of the investigation for liquid metals. Improved agreement is also obtained for other fluids, if an accurate velocity distribution is employed for the region next to the wall.

2. The step-like functions employed for the diffusivities do not represent the true functional relationship between the thermal and eddy diffusivities of heat; but rather, they help to clarify the region in which the thermal diffusivity is effective.

3. The lower limit of the turbulent core as determined by this investigation does not preclude the validity of the limit for cases without heat transfer, nor obviate the possibility that the limit is related to the fluid under consideration.

It is hoped that additional studies will encompass the following recommendations:

1. Ascertain the effect of any gas entrainment. This might be accomplished by reducing the entrained gas to a minimum and then determining the effect of controlled volumes of gas on the heat transfer coefficient.

2. Measure the velocity and temperature distributions of a liquid metal flowing turbulently in a pipe with constant heat flux,

from which their respective gradients can be accurately obtained.

3. Ascertain the effect of employing only a laminar-buffer or transition region, and turbulent core with an improved velocity distribution in the turbulent core.

4. Explore further the effect of axial conduction. The term $\overline{u'T'}$ can be measured for a gaseous material flowing turbulently in a pipe; thus providing a bound for estimation of axial conduction.

APPENDICES

APPENDIX I

PREDICTION OF NUSSELT NUMBERS BASED ON MARTINELLI'S MODEL WITH THE MOLECULAR SHEAR INCLUDED IN THE TURBULENT CORE

The question as to whether the molecular shear should be considered in the turbulent core was analyzed by Carl Gazley, Jr. in the discussion of Martinelli's work (8). He re-evaluated the resistance of the turbulent core by considering both the molecular shear and the molecular conduction. This resulted in a correction factor F; identical with F in Martinelli's work except that

$$\frac{1}{\sigma \ Pr \ Re \ \lambda}$$

becomes

$$\frac{1}{\sigma \ Pr \ Re \ \lambda} \ (1 - \sigma \ Pr)$$

To accurately determine the contribution of the molecular shear in the turbulent core the necessary equations for prediction of heat-transfer coefficients in the form of Nusselt numbers were developed for fully developed turbulent flow in pipe and in parallel plates. The resulting equation was solved by utilizing a Remington Rand Model ERA 1101 digital computer. An analytic expression was used for the laminar layer. The

trapezoidal rule was used for the buffer layer and turbulent core with twenty and thirty intervals respectively. Results of these calculations for smooth surfaces are compared with Martinelli's values in Table 10. Since the differences for flow in circular pipes are less than three per cent, the molecular shear may be neglected in the turbulent core. Note the larger error for flow between parallel plates. Table 6 compares Nusselt numbers for Pr = 0.01 calculated from the velocity distribution as measured by Deissler (10) and Laufer (33). Deissler's distribution lowered the predictions slightly, while the predictions based on Laufer's distribution were lowered approximately twenty per cent. In addition, the roughness encountered by Brown, et al, (28), is simulated in the calculations and the results, as shown, were found to be six to twelve per cent higher than for a smooth surface. It may be of interest to note that a complex analytical solution can be obtained for this development.

Table 10. Effect of the Molecular Shear in the Turbulent Core on Predicted Nusselt Numbers - Martinelli's Model

Pr	Re x 10^{-3}	Pe	Pipe		Plates	
			Nu	Nu_M	Nu	Nu_M
0.005	5	25	7.17		9.12	
0.005	10	50	7.65		9.93	
0.005	30	150	8.77		10.9	
0.005	100	500	11.5		12.8	
0.005	300	1,500	17.3		17.1	
0.005	1,000	5,000	32.0		28.3	
0.01	5	50	7.41		9.24	
0.01	10	100	8.14	7.97	10.2	11.2
0.01	30	300	10.1		11.8	
0.01	100	1,000	14.9	14.5	15.3	18.3
0.01	30	3,000	24.9		23.0	
0.01	1,000	10,000	50.3	48.7	42.6	54.0
0.025	5	125	8.06		2.95	
0.025	10	250	9.47		3.53	
0.025	30	750	13.5		5.19	
0.025	100	2,500	23.4		9.38	
0.025	300	7,500	43.9		18.2	
0.025	1,000	25,000	96.7		41.3	
0.05	5	250	9.01			
0.05	10	500	11.3		4.32	
0.05	30	1,500	18.2		7.18	
0.05	100	5,000	35.0		14.4	
0.05	300	15,000	70.3		29.7	
0.05	1,000	5,000	163.		70.5	
0.10	5		10.6			
0.10	10		14.4	14.0		
0.10	30		25.6			
0.10	100		53.9	53.0		
0.10	300		114.			
0.10	1,000		276.	271.		
0.10	3,000		641.			
0.10	10,000		1660.			
0.70	5	3,500	20.7		8.52	
0.70	10	7,000	32.7	31.2	13.9	34.0
0.70	30	21,000	71.8		31.3	
0.70	100	70,000	180.	179.	79.6	183.
0.70	300	210,000	427.		191.	
0.70	1,000	700,000	1130.	1128.	512.	1160.

Subscript M - Martinelli

APPENDIX II

PREDICTION OF NUSSELT NUMBERS BASED ON VAN DRIEST'S VELOCITY DISTRIBUTION

For turbulent flow near a smooth wall, van Driest derived the following velocity distribution for $\tau = \tau_w$:

$$\frac{\partial u^+}{\partial y^+} = \frac{2}{1 + \sqrt{1 + 4k^2 (y^+)^2 [1 - \exp(\frac{-y^+}{A^+})]^2}} \qquad (42)$$

for $0 \leq y^+ \leq 60$. This can be modified for $\tau = \tau_w(1 - \frac{y^+}{R^+})$ to yield

$$\frac{\partial u^+}{\partial y^+} = \frac{2(1 - \frac{y^+}{R^+})}{1 + \sqrt{1 + 4K^2(y^+)^2 (1 - \frac{y^+}{R^+}) [1 - \exp(-\frac{y^+}{A^+})]^2}} \qquad (43)$$

To fit Nikuradse's smooth-wall data K = 0.4 and $A^+ = 27$. For $y^+ \geq 60$, $u^+ = 5.5 + 2.5 \ln y^+$. In this analysis the field of flow is divided into two regions and discussed accordingly.

Laminar - Buffer Layer.--In this region both the molecular and eddy terms are considered. In addition, the shear and the heat transfer rate are linear as stated in Equations 6 and 16 respectively. Equation 13, for $0 \leq y^+ \leq 60$, becomes

$$\int_0^{\theta} d\theta = T^* \int_0^{y^+} \frac{(1 - \frac{\phi}{R^+})}{\frac{1}{Pr} + \frac{\varepsilon_H}{\nu}} d\phi \qquad (44)$$

From Equation 12

$$\frac{\varepsilon_M}{\nu} = \frac{\left(1 - \frac{y^+}{R^+}\right)}{\frac{du^+}{dy^+}} - 1 \tag{45}$$

Therefore,

$$\frac{\varepsilon_H}{\nu} = \sigma \frac{\varepsilon_M}{\nu} = \sigma \left[\frac{\left(1 - \frac{y^+}{R^+}\right)}{\frac{du^+}{dy^+}} - 1 \right] \tag{46}$$

Substitution into Equation 44 yields

$$\int_0^\theta d\theta = \frac{T^*}{\sigma} \int_0^{y^+} \frac{1 - \frac{\xi}{R^+}}{\frac{1}{\sigma Pr} - 1 + \frac{\left(1 - \frac{\xi}{R^+}\right)}{\frac{du^+}{dy^+}}} d\xi \tag{47}$$

Turbulent Core.--The effective magnitude of α is considered negligible compared to ε_H and ν has been shown to be negligible compared to ε_M. The shear and heat transfer rate are linear as stated in Equations 6 and 16 respectively. Equation 13, for $y^+ \geq 60$, becomes

$$\int_{\theta_I}^{\theta} d\theta = T^* \int_{60}^{y^+} \frac{\nu \left(1 - \frac{\xi}{R^+}\right)}{\varepsilon_H} d\xi \tag{48}$$

From Equation 12

$$\frac{\varepsilon_M}{\nu} = \frac{\left(1 - \frac{y^+}{R+}\right)}{\frac{du^+}{dy^+}} - 1 \tag{49}$$

Since $u^+ = 5.5 + 2.5 \ln y^+$ in the turbulent core, then

$$\frac{\varepsilon_M}{\nu} = \frac{\nu\left(1 - \frac{y^+}{R+}\right)y^+}{2.5} \tag{50}$$

Therefore,

$$\frac{\varepsilon_H}{\nu} = \sigma \frac{\varepsilon_M}{\nu} = \sigma\left[\frac{\nu\left(1 - \frac{y^+}{R+}\right)y^+}{2.5}\right] \tag{51}$$

Substitution into Equation 48, yields

$$\int_{\theta_I}^{\theta} d\theta = T^* \frac{2.5}{\sigma}\int_{60}^{y^+} \frac{dy^+}{y^+} \tag{52}$$

Hence,

$$\theta = \theta_I + T^* \frac{2.5}{\sigma} \ln \frac{y^+}{60} \tag{53}$$

Equations 47 and 53 were substituted into Equation 39 to obtain the Nusselt number. The resulting expression was integrated numerically. Table 6 presents a comparison of these results with corresponding

values obtained by using the universal velocity distribution. For Pr = 0.02 the different velocity distributions yield essentially the same Nusselt number. The remaining calculations indicate that the role of the velocity distribution near the wall becomes more important with increasing Prandtl numbers. Figure 5, which utilizes a comparison of experimental data and Rannie's theoretical predictions for Re = 10^4 as presented in his thesis, shows the vast improvement obtained for large Prandtl numbers when the van Driest velocity distribution is employed.

Intervals and method of integration were as follows:

Range	Intervals	Method
	Velocity, u^+	
$0 \leq y^+ \leq 5$	2	Simpson's rule
$5 \leq y^+ \leq 60$	11	Trapezoidal rule
$60 \leq y^+$	20	Trapezoidal rule
	Temperature, t	
$0 \leq y^+ \leq 60$	12	Trapezoidal rule
$60 \leq y^+$	20	Trapezoidal rule
	Mean temperature, θ_m	
$0 \leq y^+ \leq 60$	12	Simpson's rule
$60 \leq y^+$	20	Simpson's rule

BIBLIOGRAPHY

1. Summerfield, M., "Recent Developments in Convective Heat Transfer with Special Reference to High-Temperature Combustion Chapters," Heat Transfer Symposium, University of Michigan, 156-169 (1953).
2. Jakob, M., Heat Transfer, Vol. I, pp. 500-521, John Wiley and Sons, Inc., New York (1956).
3. Jakob, M., Heat Transfer, Vol. II, pp. 498-517, John Wiley and Sons, Inc., New York (1957).
4. Eagle, A. and Ferguson, R. M., "The Coefficient of Heat Transfer from Tube to Water," Proceedings of Royal Society of London, A127, 540-566 (1930).
5. von Karman, T., Proceedings of the Fourth International Congress of Applied Mechanics, Cambridge, England, 1934.
6. von Karman, T., "The Analogy between Fluid Friction and Heat Transfer," Transactions of the American Society of Mechanical Engineers 61, 705-710 (1939).
7. Boelter, L.M.K., Martinelli, R.C., and Jonassen, F., "Remarks on the Analogy between Heat Transfer and Momentum Transfer," Trans. Am. Soc. Mech. Eng. 63, 447-455 (1941).
8. Martinelli, R.C., "Heat Transfer to Molten Metals," Transactions of the American Society of Mechanical Engineers 69, 947-959 (1947).
9. Lyon, R.N., "Forced Convection Heat Transfer Theory and Experiments with Liquid Metals," Oak Ridge National Laboratory 361 (1949).
10. Deissler, R. G. and Eian, C. S., "Analytical and Experimental Investigation of Fully Developed Turbulent Flow in Air in a Smooth Tube with Heat Transfer with Variable Fluid Properties," National Advisory Committee for Aeronautics, Technical Note 2926 (1952).
11. Deissler, R. G., "Analysis of Turbulent Heat Transfer, Mass Transfer and Friction in Smooth Tubes at High Prandtl and Schmidt Numbers," National Advisory Committee for Aeronautics, Tech. Note 3145 (1954).
12. Rannie, W.D., Heat Transfer in Turbulent Shear Flow, Ph.D. Thesis, California Institute of Technology (1951).
13. Reichardt, H., "Heat Transfer Through Turbulent Friction Layers," National Advisory Committee for Aeronautics, Technical Note 1047, (1940).
14. Reichardt, H., "The Principles of Turbulent Heat Transfer," National Advisory Committee for Aeronautics, Technical Note 1408 (1957).
15. van Driest, E. R., "On Turbulent Flow near a Wall," Heat Transfer and Fluid Mechanics Institute, Paper No. XII, University of California (1955).

16. Hefner, R. J., Heat Transfer to Liquid Metals Flowing Turbulently in a Pipe with Walls at Constant Temperature, M.S. Thesis, Georgia Institute of Technology (1958).
17. Ross, D., "Turbulent Flow in Smooth Pipe, A Reanalysis of Nikuradse's Experiments," The Third Midwestern Conference of Fluid Mechanics, University of Minnesota (1953).
18. Ruth, B.F. and Yang, H.H., "An Empirical Correlation of Velocity Distribution of Turbulent Fluid Flow," Journal of the American Institute of Chemical Engineers 3, 117-120 (1957).
19. Rothfus, R.R., Archer, D.H., and Sikchi, K.G., "Distribution of Eddy Viscosity and Mixing Length in Smooth Tubes," American Institute of Chemical Engineers Journal 4, 27-32 (1957).
20. Brooks, F.A. and Berggren, W.P., "Remarks on Turbulent Transfer Across Planes of Zero Momentum Exchange," Paper, University of California, Agricultural Experiment Station, Davis, California.
21. Nikuradse, J., "Gesetzmassigkeiten der Turbulenten Strömung in Glatten Rohren," Vereinigung Deutschen Ingenieurn, Verlag G.M.B.H. (1932).
22. Lykoudis, P.S. and Touloukian, Y.S., "Heat Transfer in Liquid Metals," Transactions of the American Society of Mechanical Engineers 80, 653-666 (1958).
23. Jenkins, R., "Variation of the Eddy Conductivity with Prandtl Modulus and Its Use in Prediction of Turbulent Heat Transfer Coefficients," 1951 Heat Transfer and Fluid Mechanics Institute, Stanford University (1951).
24. Page, F. Jr., Schlinger, W. G., Breaux, D.K., and Sage, B. H., "Point Values of Eddy Conductivity and Viscosity in Uniform Flow between Parallel Plates," Industrial and Engineering Chemistry 44, 428-430 (1952).
25. Schlinger, W.G., Berry, V.J., Mason, J.L., and Sage, B.H., "Temperature Gradients in Turbulent Gas Streams," Industrial and Engineering Chemistry 45, 662-666 (1953).
26. Corcoran, W.H. and Sage, B.H., "Role of Eddy Conductivity in Thermal Transport," Journal of the American Institute of Chemical Engineers 2, 251-258 (1956).
27. Isakoff, S.E. and Drew, T.B., "Heat and Momentum Transfer in Turbulent Flow of Mercury," Proceedings of the General Discussion on Heat Transfer, pp. 405-409, 479-480, Institution of Mechanical Engineers, London, and American Society of Mechanical Engineers, New York; Also Isakoff, S.E., Heat and Momentum Transfer in Turbulent Flow of Mercury, Ph.D. Thesis, Columbia University (1952).
28. Brown, H,E., Amstead, B.H. and Short, B.E., "Temperature and Velocity Distribution and Transfer of Heat in a Liquid Metal," Transactions of the American Society of Mechanical Engineers 79, 279-285 (1957).

29. Sleicher, C.A., Heat Transfer in a Pipe with Turbulent Flow and Arbitrary Wall-Temperature, Ph.D. Thesis, University of Michigan (1956). Also Sleicher, C.A., Jr. and Tribus, M., "Heat Transfer in a Pipe with Turbulent Flow and Arbitrary Wall-Temperature Distribution," Transactions of the American Society of Mechanical Engineers 79, 789-797 (1957).
30. Tribus, M. and Klein, V., "Forced Convection from Non-isothermal Surfaces," Heat Transfer, A Symposium Held at the University of Michigan During 1952, Engineering Research Institute, University of Michigan, Ann Arbor, Michigan, 211-235 (1953).
31. Laufer, J., "The Structure of Turbulence in Fully Developed Pipe Flow," National Advisory Committee for Aeronautics, Technical Note 2954 (1953).
32. Lubarsky, B. and Kaufman, S.J., "Review of Experimental Investigations of Liquid-Metal Heat Transfer," National Advisory Committee for Aeronautics, Technical Note 3336 (1955).
33. Chelemer, Harold, Effect of Gas Entrainment on the Heat Transfer Characteristics of Mercury under Turbulent Flow Conditions, Ph.D. Thesis, University of Tennessee (1955).
34. Mikheyev, M.A., Baum, V.A., Voskresensky, K.D., and Fedynsky, O.S., "Heat Transfer of Molten Metals," Proceedings of the International Conference on the Peaceful Uses of Atomic Energy (Geneva) 9, 285-289 (1956).
35. Hall, W.B. and Crofts, T.I.M., "The Use of Sodium and Sodium-Potassium Alloy as a Heat Transfer Medium," Atomics Engineering and Technology 7, 167-172, 271-273, 290 (1956)
36. Kuczen, K.D., and Bump, T.R., "Measurement of Local Heat Transfer Coefficients with Sodium-Potassium Eutectic in Turbulent Flow," Nuclear Science and Engineering 2, 181-199 (1957).
37. Seban, R.A. and Casey, D.E., "Heat Transfer to Lead-Bismuth in Turbulent Flow in an Annulus," Transactions of the American Society of Mechanical Engineers 79, 1514-1518 (1957).
38. Ewing, C.T., Seebold, R.E., Grand, J.A., and Miller, R.R., "Thermal Conductivity of Mercury and Two Sodium-Potassium Alloys," Journal of Physical Chemistry 59, 524-27 (1955).
39. MacDonald, N.C. and Quittenton, R.C., "A Critical Analysis of Metal 'Wetting' and Gas Entrainment in Heat Transfer to Molten Metals," American Institute of Chemical Engineers, Preprint No. 8, 1953.
40. Hoffman, B., Chelemer, H., Stansbury, E.E., and Boarts, R.N., "The Effect of Entrainment on the Heat Transfer Characteristics of Liquid Mercury," Brookhaven National Laboratory 2446, 21-34 (1954).
41. Nikuradse, J., "Laws of Fluid Flow in Rough Pipes," Petroleum Engineer, March, May, June, July, August (1940).

42. Trefethen, L., "Measurement of Mean Fluid Temperatures," Transactions of the American Society of Mechanical Engineers 78, 1207-1212 (1956).
43. Drew, T.B., Koo, E.C. and McAdams, W.H., "The Friction Factor for Clean Round Pipe," Trans. Am. Inst. of Chem. Eng. 28, 56-72 (1932).
44. Hoffman, H.W., "Turbulent Forced Convection Heat Transfer in Circular Tubes Containing Molten Sodium Hydroxide," Oak Ridge National Laboratory 1370 (1952).
45. Johnson, H.A., Clabaugh, W.J., and Hartnett, J.P., "Heat Transfer to Mercury in Turbulent Pipe Flow," Report of U.S. Atomic Energy Commission, Contract AT-11-1-GEN 10, Project 5, Phase II (1953).
46. Johnson, H.A., Hartnett, J.P. and Clabaugh, W.J., "Heat Transfer to Molten Lead-Bismuth Eutectic in Turbulent Pipe Flow," Final Report for U.S. Atomic Energy Commission Research, Contract No. AT-(40-1)-1061, Part 2 (1951).
47. Johnson, H.A., Hartnett, J.P. and Clabaugh, W.J., "Heat Transfer to Lead-Bismuth and Mercury in Laminar and Transi-Pipe Flow," Report for U.S. Atomic Energy Commission Research, Contract AT-11-1-GEN 10, Project 5, Phase II (1953).
48. Lubarsky, B., "Experimental Investigation of Forced-Convection Heat-Transfer Characteristics of Lead-Bismuth Eutectic," National Advisory Committee for Aeronautics, Report Memorandum E51G02 (1951).
49. Stromquist, W.K., Effect of Wetting on Heat Transfer Characteristics of Liquid Metals, Ph.D. Thesis, University of Tennessee (1953).
50. Trefethen, L.M., Heat Transfer Properties of Liquid Metals, NP-1788 Technical Information Service, U.S. Atomic Energy Commission, Oak Ridge (1950).
51. McAdams, W.H., Heat Transmission, Second Edition, p. 168, McGraw-Hill Book Co., Inc., New York, 1954.

VITA

Duane L. Franklet was born in Cristobal, Canal Zone on December 8, 1929. His wife is the former Miss Beverly Bixler of Decatur, Georgia.

In the fall of 1947 he entered the Georgia Institute of Technology as a Co-operative student in the School of Chemical Engineering. In the spring of 1952 he received his bachelor's degree. The ensuing two years were spent with the Army, after which he returned to the Georgia Institute of Technology to undertake graduate study for a Ph.D. in Chemical Engineering.